ISSCR

The STAT3 Target *Mettl8* Regulates Mouse ESC Differentiation via Inhibiting the JNK Pathway

Hao Gu,[1,2,8,]* Dang Vinh Do,[3,7,8] Xinyu Liu,[1,8] Luang Xu,[1] Yixun Su,[2,3] Jie Min Nah,[6] Yuqian Wong,[1] Ying Li,[1] Na Sheng,[5] Gebreselassie Addisu Tilaye,[2,3] Henry Yang,[1] Huili Guo,[6] Jun Yan,[5] and Xin-Yuan Fu[1,2,3,4,]*

[1]Cancer Science Institute of Singapore, National University of Singapore, Singapore, Singapore, 117599
[2]Centre for Life Sciences, National University of Singapore, Singapore, Singapore, 117456
[3]Department of Biochemistry, Yong Loo Lin School of Medicine, National University of Singapore, Singapore, Singapore, 117456
[4]Department of Biology, Southern University of Science and Technology, Shenzhen, China, 518055
[5]Model Animal Research Center, Nanjing University, Nanjing, China, 210061
[6]Institute of Molecular and Cell Biology, Singapore, Singapore, 138673
[7]Genome Institute of Singapore, Singapore, Singapore, 138672
[8]These authors contributed equally
*Correspondence: csiguh@nus.edu.sg (H.G.), csifxy@nus.edu.sg (X.-Y.F.)
https://doi.org/10.1016/j.stemcr.2018.03.022

SUMMARY

The capacity of embryonic stem cells (ESCs) to differentiate into all lineages of mature organism is precisely regulated by cellular signaling factors. STAT3 is a crucial transcription factor that plays a central role in maintaining ESC identity. However, the underlying mechanism by which STAT3 directs differentiation is still not completely understood. Here, we show that STAT3 positively regulates gene expression of methyltransferase-like protein 8 (*Mettl8*) in mouse ESCs. We found that METTL8 is dispensable for pluripotency but affects ESC differentiation. Subsequently, we discovered that METTL8 interacts with *Mapkbp1*'s mRNA, which is an intermediate factor in c-Jun N-terminal kinase (JNK) signaling, and inhibits the translation of the mRNA. Thereby, METTL8 prohibits the activation of JNK signaling and enhances the differentiation of mouse ESCs. Collectively, our study uncovers a STAT3 target, *Mettl8*, which regulates mouse ESC differentiation via JNK signaling.

INTRODUCTION

Embryonic stem cells (ESCs) are derived from the inner cell mass of the blastocyst, which comprises pluripotent cells with the potential to differentiate into all cell types of the body (Williams et al., 1988b). This capacity enables ESCs a wide utilization in regenerative medicine and cell-based therapies. Therefore, a better understanding of the underlying mechanisms that modulate the differentiation of ESCs is essential for their clinical application in the future (Chen et al., 2008).

Leukemia inhibitory factor (LIF) was found to be the key growth factor for the culture and maintenance of mouse ESCs (mESCs) *in vitro* (Smith et al., 1988; Williams et al., 1988a). LIF, a member of the interleukin-6 (IL-6) family of cytokines, binds to gp130/LIFR and results in the phosphorylation on tyrosine 705 residues of STAT3, a member of the STAT gene family identified in the interferon-induced regulatory pathways (Darnell et al., 1994; Fu et al., 1990, 1992; Schindler et al., 1992). STAT3, first identified as a transcription factor (TF) for the IL-6 family of cytokines (Akira et al., 1994; Zhong et al., 1994), was subsequently found to be crucial for ESC pluripotency (Boeuf et al., 1997; Boyer et al., 2005; Niwa et al., 1998; Raz et al., 1999; Ying et al., 2003). Conventional knockout of *Stat3* in mice results in embryonic lethality at embryonic day 6.5 (E6.5) (Takeda et al., 1997). By eliminating *Stat3* in the mouse oocytes and embryos we found that STAT3

has an essential role in inner cell mass lineage specification and maintenance, and in pluripotent stem cell identity through the OCT4-NANOG circuit (Do et al., 2013).

The c-Jun NH_2-teminal kinase (JNK) belongs to the mitogen-activated protein (MAP) kinase family, which were initially identified as ultraviolet-responsive protein kinases that activated c-Jun by phosphorylating its NH_2-terminal serine/threonine residues (Dérijard et al., 1994; Hibi et al., 1993). In response to growth factors, cytokines, and a number of environmental stresses, JNK is activated through a well-orchestrated cascade of MAP kinase activation (Jaeschke et al., 2006; Sabapathy et al., 2004). In particular, mitogen-activated kinase kinase 4 and 7, isoforms of MAP2K, directly phosphorylate and activate JNK, which in turn leads to the phosphorylation of (TF) c-Jun and switching on of transcriptional regulation exclusively through formation of complex with other TFs, such as c-fos, in the activator protein-1 complex (Davis, 2000; Weston and Davis, 2007). *JNK* is encoded by two ubiquitously expressed genes (*JNK1* and *JNK2*) and by a third gene (*JNK3*) that is selectively expressed in neurons. MAPKBP1 is a JNK binding protein and enhances the activation of JNK (Koyano et al., 1999; Lecat et al., 2012). Recent studies indicated that JNK signaling is required for lineage-specific differentiation but not stem cell self-renewal. ESCs lacking *JNK1* show transcriptional deregulation of several lineage-commitment genes and fail to undergo neuronal differentiation, as do ESCs lacking JNK
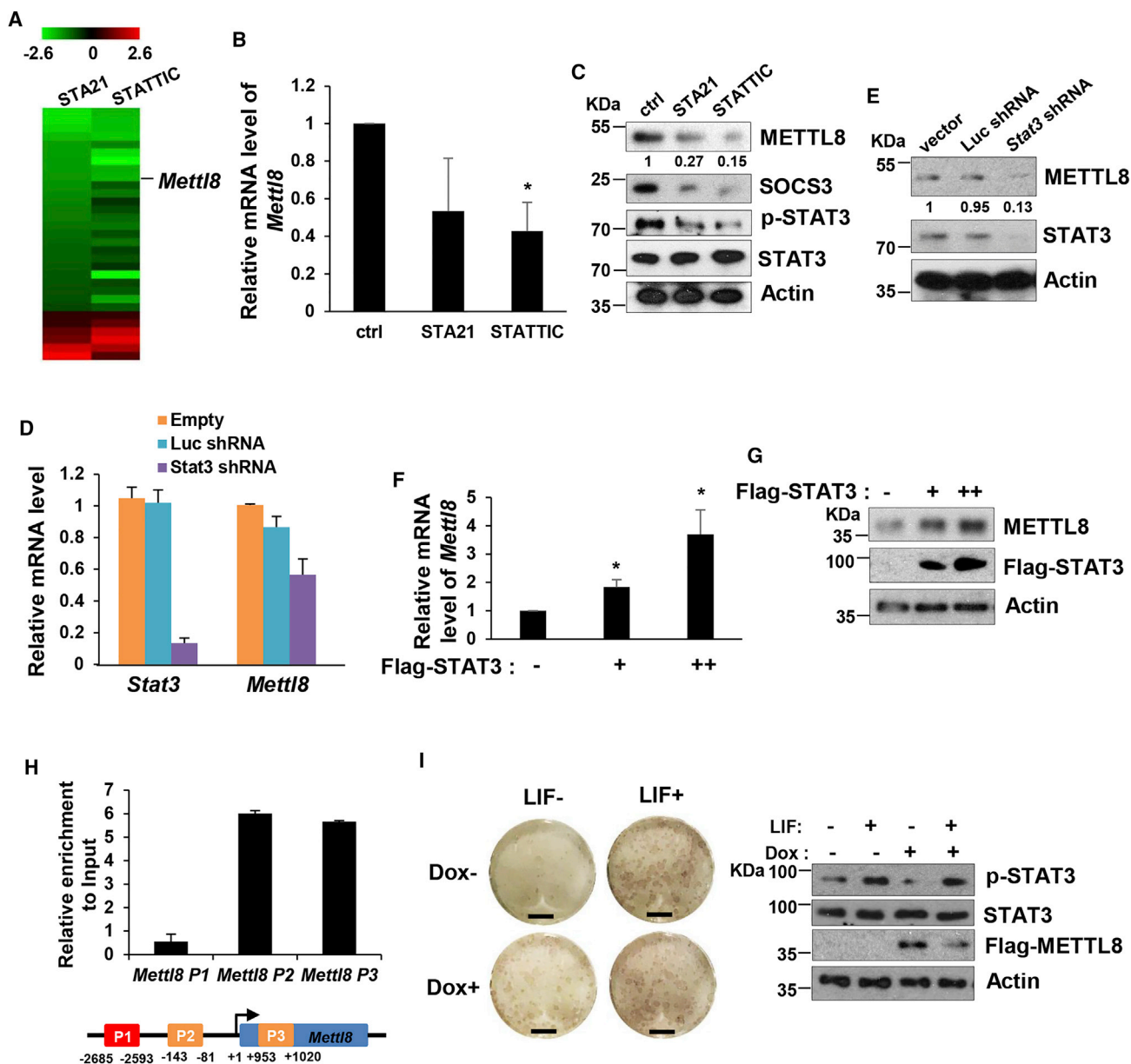
Figure 1. _Mettl8_ Is Transcriptionally Regulated by STAT3

(A) Real-time PCR was performed to screen for changes when ESCs were treated with STA-21 and STATTIC for 1 hr.

(B and C) E14 cells were treated with STA-21 and STATTIC for 6 hr and harvested. (B) Total RNAs were extracted and followed by real-time PCR analysis. Data are shown as the mean ± SD from three independent experiments. *p < 0.05. (C) Cell lysates were analyzed by western blot. The value of each band was calculated from three independent replicates and indicates the relative expression level after normalizing to the loading control actin.

(D) Knockdown _Stat3_ in E14 cells resulted in downregulation of _Mettl8_ mRNA. Data are shown as the mean ± SD from three independent experiments.

(E) Knockdown _Stat3_ in E14 cells resulted in downregulation of METTL8 protein. The value of each band was calculated from three independent replicates and indicates the relative expression level after normalizing to the loading control actin.

(F and G) E14 cells were transfected with Flag-vector or Flag-tagged STAT3 at increasing concentrations. (F) Total RNAs were extracted followed by real-time PCR analysis. Data are shown as the mean ± SD from three independent experiments. *p < 0.05. (G) Cell lysates were analyzed by western blot.

(legend continued on next page)

pathway scaffold proteins (Xu and Davis, 2010). Studies also found that JNK binds to a large set of active promoters during the differentiation of stem cells and results in histone 3 phosphorylation on chromatin (Tiwari et al., 2011). It is also reported that JNK regulates STAT3 activity via its Ser-727 phosphorylation, showing the crosstalk between STAT3 and JNK pathways (Lim and Cao, 1999).

In this study, we further investigate how STAT3 integrate to the core regulatory circuit in ESC pluripotency and differentiation, and identify *Mettl8* as a downstream target of STAT3 in mESCs. We discover the role of METTL8 as a negative regulator of JNK signaling in stem cells. Our results provide insights into the crosstalk between STAT3 and JNK signaling during stem cell differentiation.

RESULTS

Mettl8 Is a Direct Target of STAT3 in mESCs

In this study, we further investigated how STAT3 crosstalk with other potential pathways in ESC pluripotency. Therefore, we screened for unknown factors that were regulated by STAT3 using ESCs treated with STAT3 inhibitors STA-21 and STATTIC (Schust et al., 2006; Song et al., 2005). Real-time PCR results obtained from screening for a library of 200 epigenetic candidates led us to identify *Mettl8* (Figure 1A). We found that the mRNA levels of *Mettl8* were downregulated after the two-inhibitor treatment (Figure 1B). Meanwhile, we checked *Mettl8*'s protein level, which was also inhibited by STA-21 and STATTIC (Figures 1C and S1).

To further confirm that *Mettl8* is a target of STAT3, we reduced *Stat3* transcript levels by employing *Stat3* small hairpin RNAs (shRNAs), and found that both *Mettl8* mRNA and protein levels in ESCs were reduced (Figures 1D and 1E). Next we validated this result with STAT3 overexpression in mESCs. When STAT3 was overexpressed, both *Mettl8* mRNA and protein levels were upregulated (Figures 1F and 1G). To examine whether STAT3 regulates *Mettl8* directly or indirectly, we used bioinformatics, and identified three possible STAT3 binding sites on *Mettl8* gene at −2,672, −83, and 1,020 bp (PROMO software). We then performed chromatin immunoprecipitation (ChIP) assay using the pY705-STAT3-specific antibody. We found the highest enrichment in a promoter region at −83 bp and a proximal enhancer at 1,020 bp of *Mettl8* gene (Figure 1H). These results show that STAT3 directly interacts with the regulatory regions of the *Mettl8*. Taken together,

our evidence demonstrate STAT3 directly and positively regulates *Mettl8* expression in pluripotent cells.

To further figure out whether METTL8 exerts a key function downstream of STAT3 in ESCs, we created inducible METTL8 overexpression mESCs. After LIF withdrawal ESCs became differentiated, but METTL8 overexpression rescued this phenomenon and showed more ESC colonies stained positive for alkaline phosphatase (AP) (Figure 1I), suggesting that METTL8 mediates the role of STAT3 in pluripotent cells.

### METTL8 Is Dispensable for the Maintenance of Pluripotency in mESCs

To examine the function of METTL8 in mESCs, we first induced mESCs to differentiation by retinoic acid (RA) treatment and found both mRNA and protein levels of *Mettl8* were reduced (Figures 2A and 2B). Similarly, during embryoid body (EB) formation, *Mettl8* was also significantly downregulated from day 6 onward and barely detectible at days 9–15 (Figures 2C and 2D). These data imply that expression of *Mettl8* is correlated with the pluripotent state of ESCs, thus we next evaluated the direct effect of METTL8 on ESC pluripotency. However, when *Mettl8* was knocked out, the morphology of ESCs showed no difference from the wild-type cells, which were positive in AP staining (Figure 2E). Moreover, mRNA and protein expressions of key pluripotent genes were not changed in *Mettl8* deficient or overexpressed mESCs (Figures 2F, 2G, 2H, and S2A), and *Mettl8* overexpression or knockout had little impact on the clonogenicity of mESCs (Figures 2I and 2J). However, when cultured in sub-optimal conditions, self-renewal of *Mettl8*-null ESCs is weakened (Figure 2J). These results suggested METTL8 is dispensable for ESC pluripotency when *Mettl8*-null ESCs are cultivated in normal conditions but might play a role in ESC differentiation.

METTL8 Inhibits mESC Differentiation

We next examined the function of METTL8 in differentiation assay of ESCs. Interestingly, after 10 days of EB formation, the numbers of AP-positive ESCs decreased in the *Mettl8* knockout (KO) group (Figures 2K and S2B). Consistently, more ectopic expression of METTL8 led to higher AP-positive numbers from EBs (Figure 2L), which suggests that METTL8 impedes mESC differentiation. Then global gene transcriptome profiling was performed with whole-genome cDNA microarray to find out the genes with significant changes between *Mettl8* or scramble small interfering

(H) Bioinformatic analysis identifies three possible STAT3 binding sites on *Mettl8* gene labeled as P1, P2, and P3. Data are shown as the mean ± SD from three independent experiments.
(I) Inducible Flag-METTL8 overexpression E14 cells were treated with or without doxycycline and culture in mediums with or without LIF for 6 days. Then colonies were stained for AP activity and cell lysates were analyzed by western blot. Scale bars, 0.5 cm.
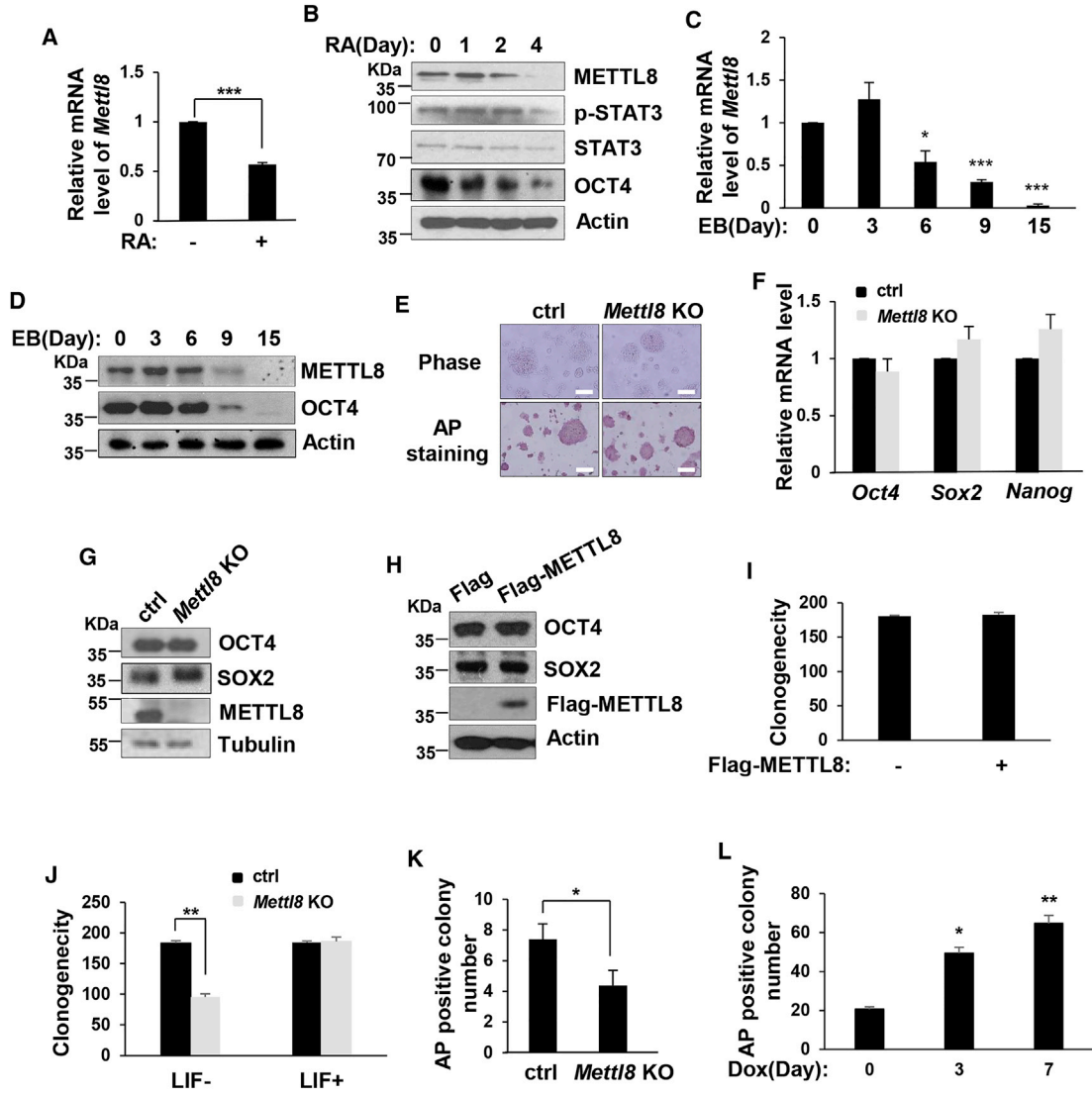
Figure 2. METTL8 Affects ESCs Differentiation Rather Than Pluripotency

(A) Total RNAs were extracted from E14 cells treated with RA for 0 or 4 days, followed by real-time PCR analysis. Data are shown as the mean ± SD from three independent experiments. ***p < 0.001.

(B) E14 cells were treated with RA for the indicated times and cell lysates were analyzed by western blot.

(C and D) E14 cells were subjected to EB formation and cells were harvested at the indicated times. (C) Total RNAs were extracted followed by real-time PCR analysis. Data are shown as the mean ± SD from three independent experiments.*p < 0.05, ***p < 0.001. (D) Cell lysates were analyzed by western blot.

(E) *Mettl8* KO and control E14 cells were stained for AP activity and pictures were taken. Scale bars, 100 μm.

(F) Total RNAs were extracted from *Mettl8* KO and control E14 cells followed by real-time PCR analysis. Data are shown as the mean ± SD from three independent experiments.

(G) Cell lysates of *Mettl8* KO and control E14 cells were analyzed by western blot.

(H and I) E14 cells were transfected with Flag-vector or Flag-tagged METTL8 and (H) 48 hr later cell lysates were analyzed by western blot. (I) Colony-forming assays were performed and the number of AP-positive colonies was counted.

(J) *Mettl8* KO and control cells were cultured under normal condition or LIF deprivation for 4 days. Then colony-forming assays were performed and the number of AP-positive colonies was counted. **p < 0.01.

(K) *Mettl8* KO and control E14 cells were subjected to EB formation for 7 days. EBs were trypsinized and re-plated into gelatin-coated dished. After 3 days culture in ESC medium, colonies were stained for AP activity and AP-positive colonies were counted. Data are shown as the mean ± SD from three independent experiments. *p < 0.05.

(legend continued on next page)

RNA (siRNA) mESCs (Table S1). We found that 353 genes were upregulated (>2-fold) and 89 transcripts were downregulated (>2-fold) after *Mettl8* depletion. To define discreet functional clusters of common gene regulation, we performed a hierarchical clustering of our microarray data. This analysis yielded four discernable clusters of commonly regulated genes with two each associated with up- and downregulation (Figure S2C). Overall upregulated gene clusters were associated with developmental capacity. When we performed gene ontology we found that these upregulated genes are enriched for gene ontology terms such as developmental process and cellular differentiation. Particularly, we found some key upregulated lineage genes such as *Pax6, Gata6, T*, and *Hand1*, which have been reported to be upregulated during mESC differentiation (Figure S2C). We also examined the global gene expression changes using RNA sequencing (RNA-seq) comparing the transcriptome from ESCs with either *Mettl8* or scramble siRNA. We found that 198 genes were downregulated (>2-fold) and 1,353 transcripts were upregulated (>2-fold) after *Mettl8* depletion (Figure S2D). Consistent with microarray data, we also found key upregulated developmental genes such as *Pax6, Gata6, T*, and *Hand1*, and then used real-time PCR to validate the increase in mRNA expression of these genes (Figure S2E). Taken together, these results suggested that METTL8 indeed inhibits ESC differentiation, possibly by suppressing expression of some key developmental genes.

METTL8 Functions in Somatic Reprogramming

Given the role of METTL8 in the regulation of ESC differentiation, we sought to further explore its functions in induced pluripotent stem cells (iPSCs) and determine whether METTL8 also regulates somatic reprogramming. Firstly, using the well-established iPSC mouse model (Carey et al., 2010), we found both mRNA and protein levels of *Mettl8* were increased during cellular reprogramming after inducing OSKM (OCT4, SOX2, KLF4, and MYC) in MEF cells (Figures 3A and 3B), indicating that METTL8 may facilitate reprogramming. To test this hypothesis, we crossed *Mettl8* KO with inducible OSKM strain to introduce *Mettl8* KO MEF cells along with OSKM induction. *Mettl8* deficiency indeed resulted in a decreased iPSC colony formation (Figure 3C). These *Mettl8* KO iPSC colonies shared a similar morphology with the wild-type ones (Figure 3D). In addition, RT-PCR analysis revealed that all of the randomly picked *Mettl8* KO MEF-derived colonies expressed endogenous ESC marker genes, including *Oct4, Sox2, Nanog, Rex1, Fbx15*, and *Esg1* (Figure 3E). Immunofluorescence analysis also showed that these colonies were positive for pluripotent markers OCT4 and SOX2 (Figure 3F). Together our results suggest that METTL8 play its role in somatic reprogramming.

METTL8 Interacts with *Mapkbp1* mRNA

As we discovered simultaneously that METTL8 interacts with mRNAs (Xu et al., 2017), to further understand the mechanism of METTL8 in pluripotent cells, we sought to identify METTL8-interacting RNAs by photoactivatable ribonucleoside-enhanced crosslinking and immunoprecipitation (PAR-CLIP) assay (Hafner et al., 2010) (Figure 4A). The subsequent analysis indeed revealed that mRNAs are potential METTL8 protein interacting partners, which account for a large proportion of the binding peaks (Table S2). This result was matched with the subcellular distribution of METTL8 protein that it is mainly located at the cytoplasm where most mature mRNA resides (Figure 4B). To elucidate the mechanism by which METTL8 works through its mRNA partners, we chose *Mapkbp*1 mRNA from the candidates for detailed investigation, and RNA immunoprecipitation (RIP) assay was performed. We discovered that *Mapkbp1* mRNAs were enriched in Flag-tagged METTL8 expression sample, which confirmed METTL8 protein's ability to bind *Mapkbp*1 mRNA (Figure 4C). The endogenous complex between METTL8 protein and *Mapkap1* mRNA was also detected by RIP assay using METTL8 antibody (Figure 4D). In addition, the interaction of METTL8 with *Mapkbp1* mRNA was further verified by affinity pull-down of endogenous *Mapkbp*1 mRNA using a biotinylated RNA antisense probe to *Mapkbp*1 mRNA (Figure 4E).

METTL8 Inhibits *Mapkbp1* mRNA Translation

To clarify the influence of METTL8 protein on its interacting partner, we next tested the expression level of *Mapkbp1* mRNA after knocking out *Mettl8* in ESCs. The results showed no significant change between *Mettl8* KO and control cells (Figure 5A). Similar results were obtained when METTL8 was overexpressed in HEK293T cells (Figure 5B), demonstrating that METTL8 does not affect mRNA levels of *Mapkbp1*. Thus, we then checked the protein level of *Mapkbp1*, and found a higher expression of MAPKBP1 protein in *Mettl8* KO cells (Figures 5C and S3A). Based on this data, we speculated that METTL8 decreases the protein

(L) Inducible METTL8 overexpression E14 cells were treated with or without doxycycline and subjected to EB formation for 7 days, or treated with doxycycline for the first 3 days of EB formation. Then EBs were trypsinized and re-plated into gelatin-coated dishes. After 3 days culture in ESC medium, colonies were stained for AP activity and AP-positive colonies were counted. Data are shown as the mean ± SD from three independent experiments. *p < 0.05, **p < 0.01.
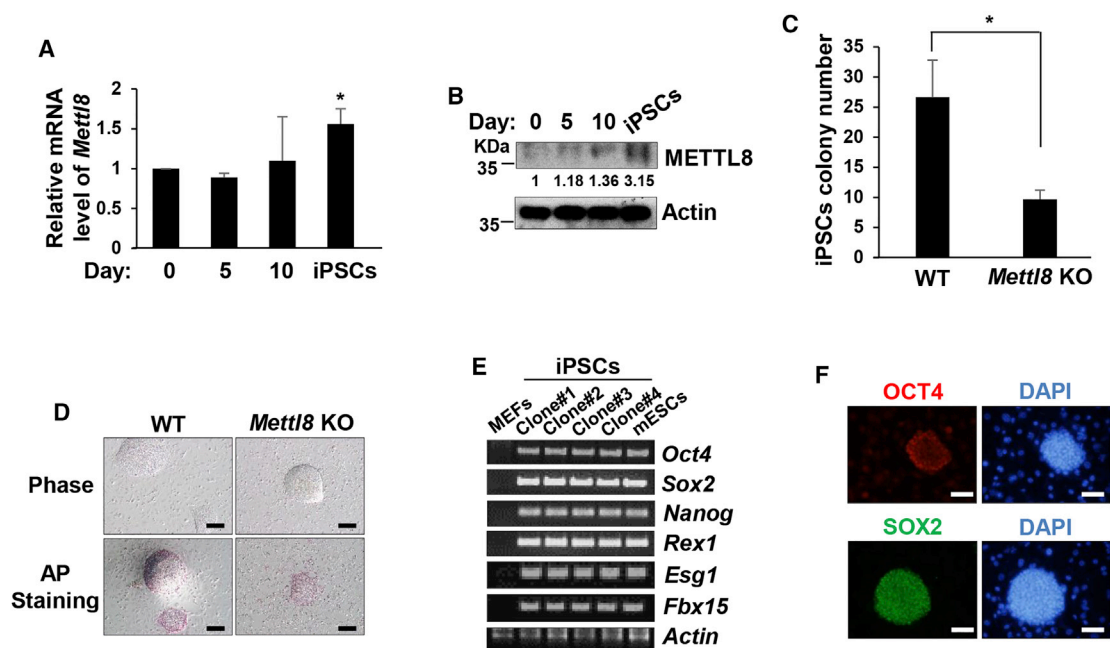
Figure 3. METTL8 Functions in Somatic Reprogramming

(A) Total RNA was extracted from OSKM-inducible MEF cells treated with doxycycline on days 0, 5, and 10, and iPSCs followed by real-time PCR analysis. Data are shown as the mean ± SD from three independent experiments. *p < 0.05.

(B) Cell lysis from OSKM-inducible MEF cells treated with doxycycline on days 0, 5, and 10, and iPSCs and analyzed by western blot. The value of each band was calculated from three independent replicates and indicates the relative expression level after normalizing to the loading control actin.

(C) Wild-type and *Mettl8* KO OSKM-inducible MEF cells were treated with doxycycline and induced for iPSCs. After 20 days, numbers of iPSC colonies were counted. Data are shown as the mean ± SD from three independent experiments. *p < 0.05.

(D) Wild-type and *Mettl8* KO iPSCs were stained for AP activity and pictures were taken. Scale bars, 100 μm.

(E) Total RNA from MEF cells, E14 cells, and the indicated *Mettl8* KO iPSC colonies were subjected to RT-PCR analysis for detection of expression of endogenous *Oct4, Sox2, Nanog, Rex1, Fbx15,* and *Esg1*. Actin was used as an internal control.

(F) *Mettl8* KO iPSC colonies were subjected to immunofluorescence for analysis of endogenous OCT4 and SOX2 expression. Scale bars, 50 μm.

stability of MAPKBP1. However, when ESCs treated with cycloheximide (CHX) and protein synthesis was blocked, the degradation rate of MAPKBP1 protein showed no significant change between *Mettl8* KO and control cells (Figure 5D), indicating that protein stability of MAPKBP1 was not affected. Then we hypothesized that METTL8 may influence translation, and to directly test the possibility, *Mettl8* KO and control ESC lysates were subjected to polysome profiling by fractionation through sucrose gradients. The lightest components sedimented at the top (fractions 1 and 2), small (40S) and large (60S) ribosomal subunits and monosomes (80S) located in fractions 3 to 8, and larger polysomes in fractions 9 to 15 (Figure 5E). *Mettl8* KO did not change global polysome distribution profiles, indicating that it did not affect global translation (Figure 5E). After isolating RNA from each fraction, real-time PCR analysis indicated that *Mapkbp1* mRNA in *Mettl8* KO cells was abundant in fractions 12 to 15, while in control cells it

was abundant in fractions 4 to 6 and 11 to 13 (Figure 5F). The result indicates that silencing *Mettl8* leads to *Mapkbp1* mRNA distribution shifting toward larger polysomes and thus promotes translation. As a negative control, actin mRNA did not show that shift (Figure 5F). Taken together METTL8 affects *Mapkbp1* expression through binding to *Mapkap1* mRNA and inhibiting its translation.

METTL8 Inhibits JNK Signaling in mESCs

To further understand the consequences of the interaction between METTL8 and *Mapkbp1* mRNA, we next investigated the role of MAPKBP1 in ESCs. We induced differentiation of ESCs by RA treatment and found mRNA levels of *Mapkbp1* were not changed during the process (Figure 6A). This result was expected as we postulate that mRNA expression of *Mapkbp1* is not affected by METTL8. However, an increase of MAPKBP1 protein level was observed after RA treatment, accompanying the emergence of
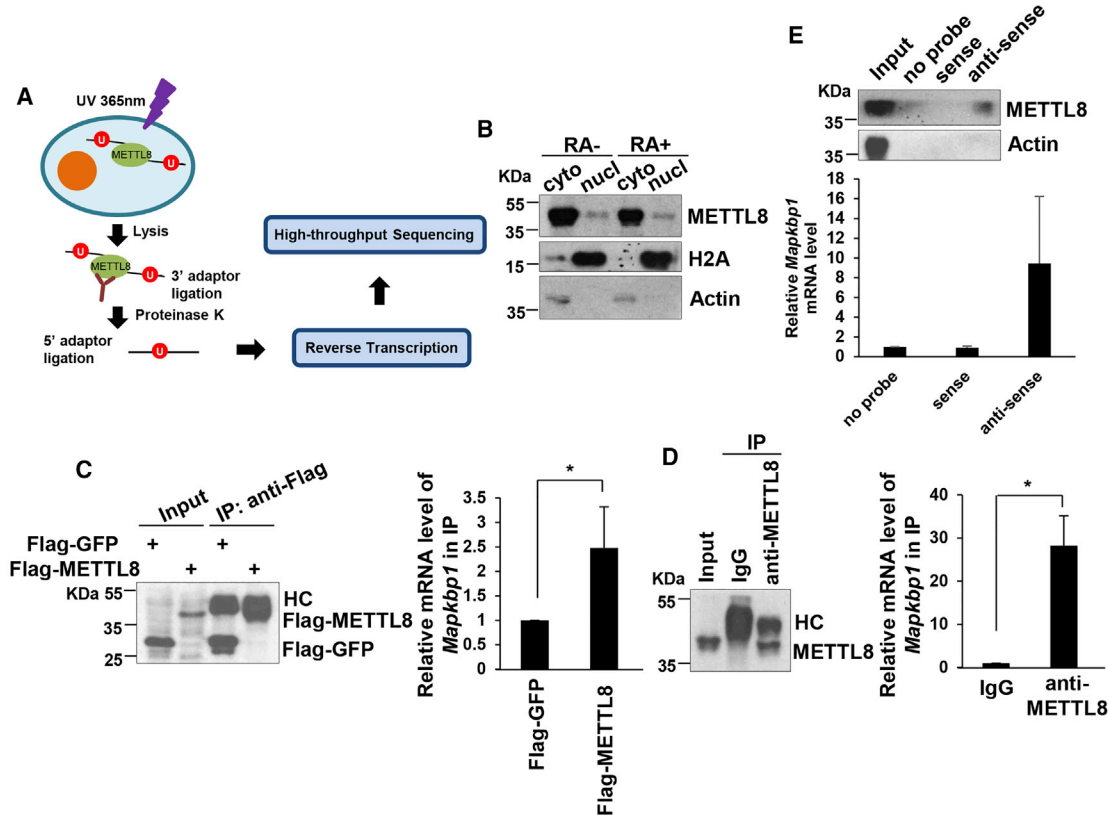
Figure 4. METTL8 Binds to *Mapkbp1* mRNA

(A) Schematic illustration of PAR-CLIP assay.

(B) E14 cells were harvested and subjected to cell fractionation. Each fraction was collected and analyzed by western blot.

(C) HEK293T cells were transfected by the indicated plasmids. After 48 hr cells were harvested and subjected to RIP with flag antibody. Total RNAs were extracted followed by real-time PCR analysis. Actin was used as an internal control. Data are shown as the mean ± SD from three independent experiments. *p < 0.05.

(D) E14 cells were harvested and subjected to RIP with METTL8 antibody or isotype-matched immunoglobulin G (IgG). Total RNAs were extracted and relative level of *Mapkbp1* mRNA was analyzed by quantitative real-time PCR. Actin was used as an internal control. Data are shown as the mean ± SD from three independent experiments. *p < 0.05.
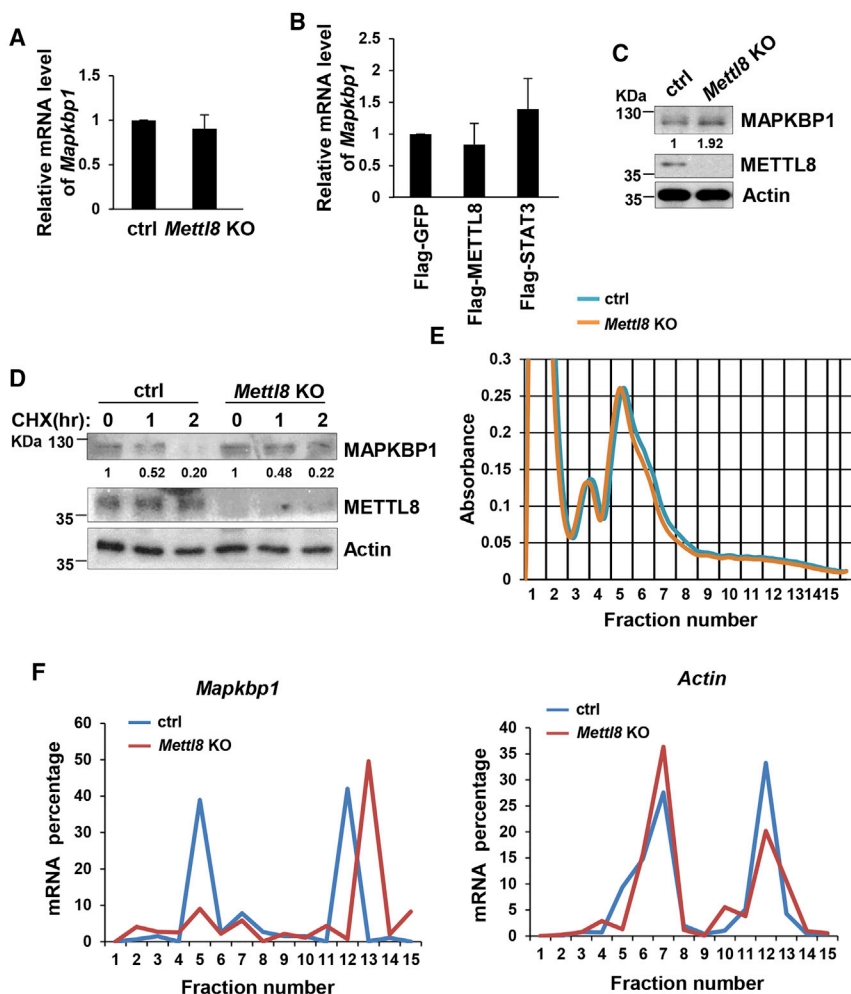
(E) E14 cells were harvested and cell lysates were then incubated with *in-vitro*-synthesized biotin-labeled sense or antisense *Mapkbp1* mRNA probes for biotin pull-down assay, followed by western blot analysis.

phosphorylated JNK, which was not detectable in that pluripotent state (Figures 6B and S3B). Moreover, the expression levels of both MAPKBP1 and phosphorylated JNK were higher in *Mettl8* KO cells than control cells (Figures 6B and S3B). These results suggest that *Mettl8* KO enhances JNK signaling during differentiation. To further confirm the hypothesis, we employed another model of ESC differentiation, EB formation, and also found an enhanced JNK signal in *Mettl8* KO EBs (Figure 6C). By contrast, although level of phosphorylated JNK protein was quite low in MEFs, during somatic reprogramming MAPKBP1 and phosphorylation of JNK showed a decreasing tendency and still appeared at higher levels in *Mettl8* KO cells (Figure 6D). Finally we performed the JNK assay and confirmed that the enzyme activity of JNK was

indeed enhanced in *Mettl8*-deficient cells (Figure 6E). Taken together, METTL8 inhibits JNK signaling through MAPKBP1 in mESCs.

The METTL8-MAPKBP1-JNK Pathway Suppresses ESC Differentiation

To further validate that METTL8 regulates the JNK pathway during differentiation, we next performed *in vitro* differentiation assays in ESCs. According to a previous study, JNK proteins are mostly enriched for regulating genes involved in nervous and cardiovascular system development (Tiwari et al., 2011). Therefore we next subjected mESCs to neural and cardiac differentiation *in vitro*. When *Mettl8* was silenced, neuronal differentiation was enhanced, which, however, showed no significant change in *Mettl8* and

Mapkbp1 double KO (DKO) cells (Figures 7A and S4A). Similarly, cardiac differentiation of *Mettl8* KO cells followed the same pattern in *Mettl8* and *Mapkbp1* DKO cells (Figures 7B and S4B). Moreover, we also examined markers of other germline layers, some of which were also upregulated in *Mettl8* KO cells and rescued in *Mettl8* and *Mapkbp1* DKO cells (Figures S4C and S4D). These results indicate that MAPKBP1 mediates the function of METTL8 during differentiation. Meanwhile we performed the same assays in *Mettl8* KO cells treated with JNK inhibitor SP600125, and the number of cells with *Nestin* and *Gata4* expression was consistently reduced compared with those without treatment (Figures 7C, 7D, S4E, and S4F). The expression of other lineage markers was also lower in SP600125-treated *Mettl8* KO cells (Figures S4G and S4H), indicating that METTL8-MAPKBP1 regulates ESC differentiation by the JNK pathway.

Taken together, as depicted in Figure S5A, our results unravel a pathway whereby STAT3 regulates mESC differentiation by transcriptionally activating *Mettl8*, which, in turn, inhibits JNK signaling through interaction with a key JNK modulator, *Mapkbp1* mRNA and attenuating its translation.

DISCUSSION

In this study, we identified *Mettl8* as a transcriptional target of STAT3 that mediates STAT3's functions in mESCs. According to previous studies, STAT3 responds to external cytokine LIF and then transcribes critical pluripotent factors in the nucleus, such as *Oct4* and *Nanog*. Nevertheless, it remains undefined if STAT 3 is able to regulate stem cell pluripotency or differentiation by other mechanisms. We report here that METTL8 mediates a role of STAT3 during ESC differentiation. Our results indicate that STAT3, besides modulating *Oct4* and *Nanog* expression, plays diverse roles in maintenance of ESC identity.

We found that METTL8 impedes differentiation of mESCs rather than pluripotency. Through RNA-seq and
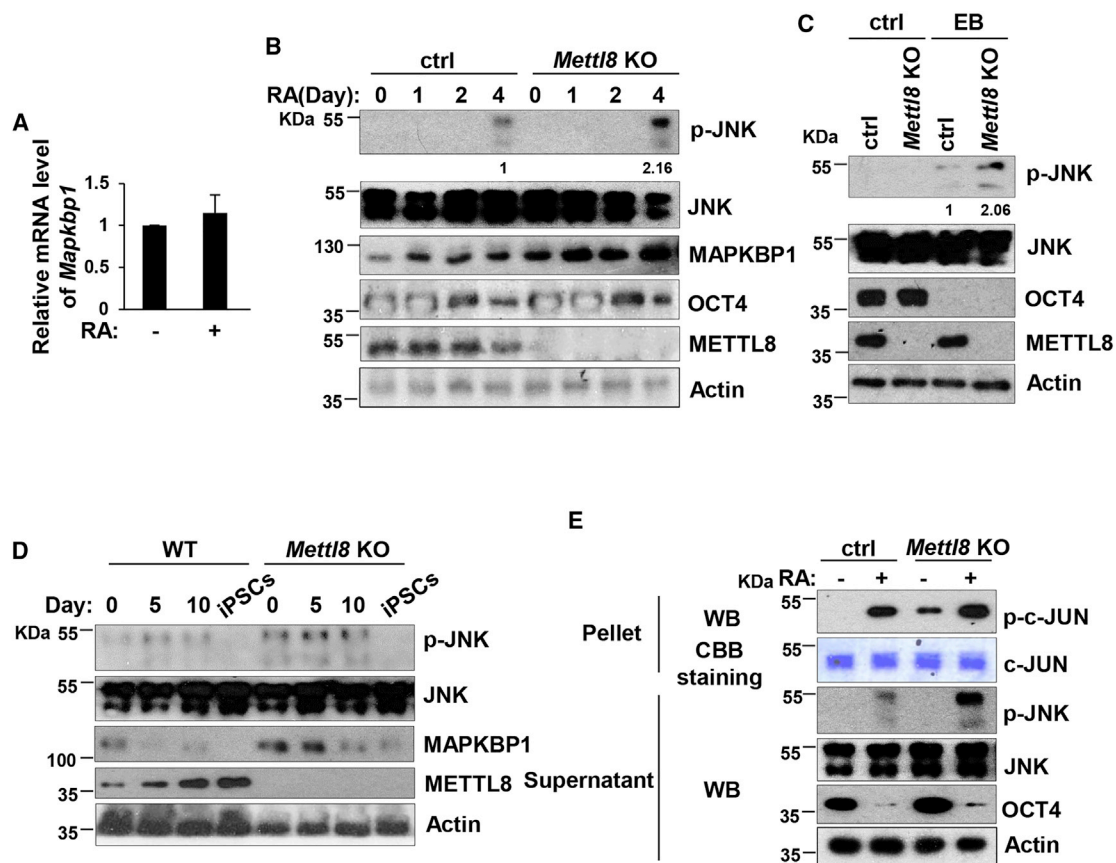
Figure 6. METTL8 Inhibits JNK Signaling in ESCs

(A) Total RNAs were extracted from E14 cells treated with RA for 0 or 4 days, followed by real-time PCR analysis. Data are shown as the mean ± SD from three independent experiments.

(B) *Mettl8* KO and control E14 cells were treated with RA for the indicated times and cell lysates were analyzed by western blot. The value of each band was calculated from three independent replicates and indicates the relative expression level after normalizing to the loading control actin.

(C) *Mettl8* KO and control E14 cells were subjected to EB formation and 21 days later cell lysates were analyzed by western blot. The value of each band was calculated from three independent replicates and indicates the relative expression level after normalizing to the loading control actin.

(D) *Mettl8* KO and control MEF cells were induced to iPSCs and collected at indicated times. Cell lysates were analyzed by western blot.

(E) *Mettl8* KO and control E14 cells were treated with RA for 0 or 4 days were harvested and cell lysates were subjected to JNK assay, followed by western blot analysis.

microarray analysis, it is discovered that lineage markers increased in *Mettl8*-deficient ESCs, while pluripotency markers showed no change. However, we think those elevated lineage genes are not a strong enough driving force for ESC differentiation. As a result, *Mettl8* KO cells maintain a pluripotent state. Nevertheless, once those *Mettl8*-deficient cells were deprived of pluripotent conditions they would be more vulnerable to differentiate. However, different to embryo lethality caused by *Stat3* deficiency, no abnormal phenotype was observed in *Mettl8* KO mice. So it needs further investigation if there is redundancy between METTL family members. One of the METTL

family genes, *Mettl3*, is also reported to bind mRNA transcripts, and inhibits mRNA stability (Geula et al., 2015).

We also used an affinity purification approach and subsequent mass spectrometry analysis to explore the interacting proteins with METTL8, and found a number of RNA binding proteins in the candidates list (Table S3). This result suggests that the binding between METTL8 and *Mapkbp1* mRNA may be not direct, and that some RNA binding proteins may mediate the interaction, which needs further investigation. In addition, mRNA of *Gata6*, which is a lineage marker, was also proved to bind to METTL8 by subsequent experiments (data not
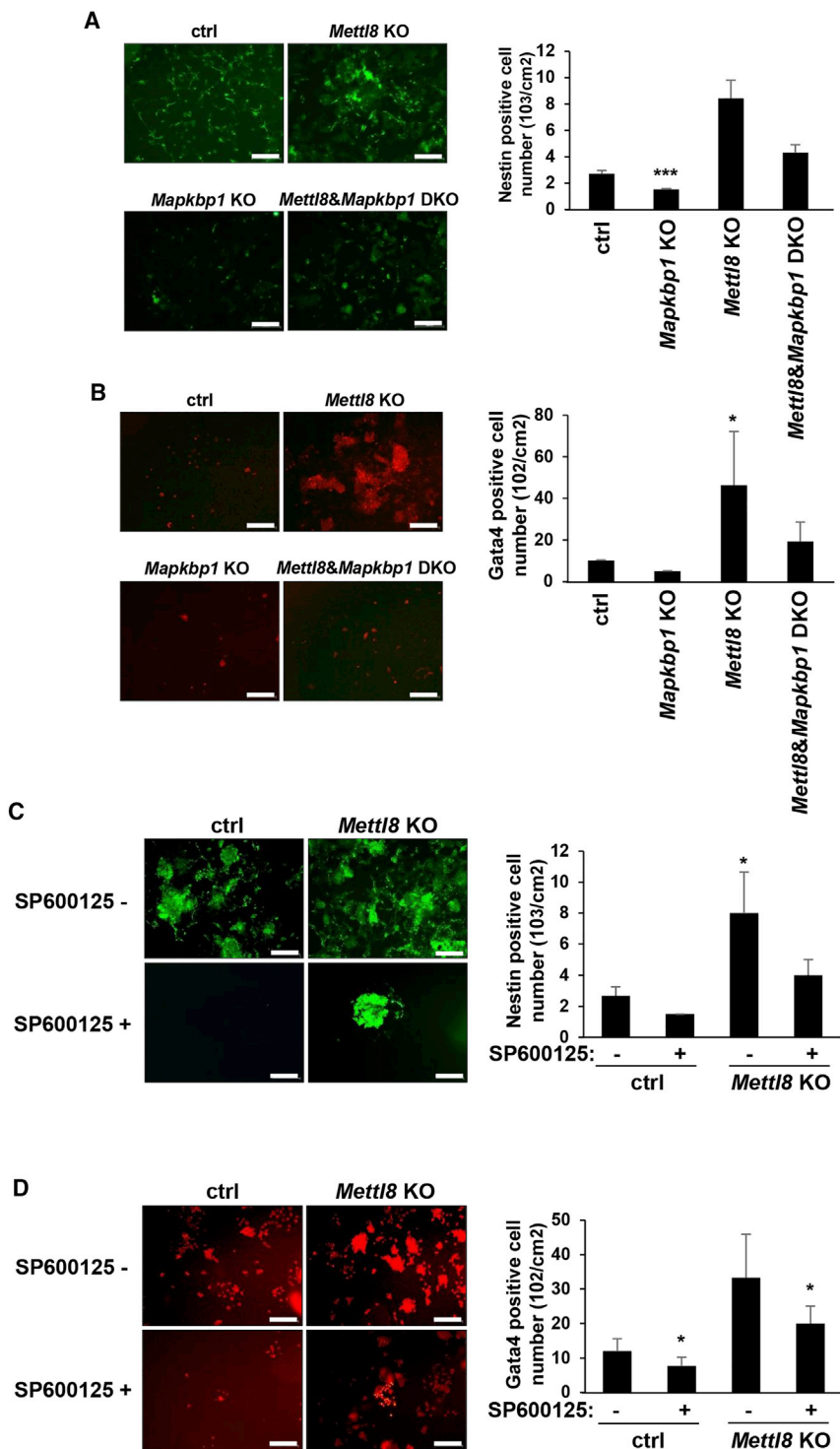
Figure 7. The METTL8-JNK Pathway in ESC Differentiation

(A) *Mettl8* KO, *Mapkbp1* KO, *Mettl8,* and *Mapkbp1* DKO, and control E14 cells, were subjected to neuron progenitor cells differentiation. Cells were stained for expression of Nestin and positive cells were counted by cytometer. Data are shown as the mean ± SD from three independent experiments. ***p < 0.001. Scale bars, 100 μm.

(B) *Mettl8* KO, *Mapkbp1* KO, *Mettl8,* and *Mapkbp1* DKO, and control E14 cells, were subjected to cardiac differentiation. Cells were stained for expression of Gata4 and positive cells were counted under fluorescence microscopy. Data are shown as the mean ± SD from three independent experiments. *p < 0.05. Scale bars, 100 μm.

(C) *Mettl8* KO and control E14 cells were treated with or without SP600125 and subjected to neuron progenitor cells differentiation. Cells were stained for expression of Nestin and positive cells were counted by cytometer. Data are shown as the mean ± SD from three independent experiments. *p < 0.05. Scale bars, 100 μm.

(D) *Mettl8* KO and control E14 cells were treated with or without SP600125 and subjected to cardiac differentiation. Cells were stained for expression of Gata4 and positive cells were counted under fluorescence microscopy. Data are shown as the mean ± SD from three independent experiments. *p < 0.05. Scale bars, 100 μm.

shown). Coincidently *Gata6* mRNA also showed an upregulation in *Mettl8* knockdown cells in both microarray and RNA-seq analysis, which suggests that METTL8 may affect differentiation through alternative factors and mechanisms.

It is reported that METTL8 causes 3-methylcytidine (m3C) modification on human mRNAs (Xu et al., 2017). METTL8 contains a conserved methytransferase domain and is predicted to have methytransferase activity. Consistently, from the PAR-CLIP data in our study, most candidate

METTL8 binding partners are mRNAs. We should further investigate if METTL8 modifies m3C on *Mapkbp1* mRNA and then causes translation inhibition. In addition, other METTL family proteins also reported to modify mRNAs. For example, METTL3 and METTL14 catalyze m(6)A RNA methylation (Liu et al., 2014), which is critical for glioblastoma stem cell self-renewal (Cui et al., 2017).

MAPKBP1 enhances JNK signaling activated by mitogen-activated protein kinase kinase 1 (MEK1) and transforming growth factor β-activated kinase 1 (Koyano et al., 1999). Given that extracellular signal-regulated kinase (ERK) signaling is a major driving force for mESC differentiation and that MEK 1 also activates ERK signaling, the crosstalk between JNK and ERK signaling is worth being further studied. Moreover, studies showed that JNK signaling is required for lineage-specific differentiation but not stem cell self-renewal (Xu and Davis, 2010), which is consistent with our finding that METTL8 affects differentiation but not the pluripotent state. It is reported that JNK signaling can induce STAT3-Ser727 phosphorylation, which is important for the transactivation potency of STAT3 (Lim and Cao, 1999). Here, we also found that, when the STAT3 pathway was inhibited, JNK phosphorylation showed a higher level. However, this phenotype became subtle in *Mettl8* KO cells, indicating that STAT3 has a feedback on JNK signaling in mESCs mediated by METTL8 (Figure S5B).

Taken together, our results identified a signaling axis STAT3-METTL8-MAPKBP1-JNK that is important for mESC differentiation and further broadens the landscape of regulatory networks in mESCs.

EXPERIMENTAL PROCEDURES

Cell Culture and RNA Interference

mESCs were maintained in Glasgow minimum essential medium supplemented with 15% fetal bovine serum (FBS), 2 mM L-glutamine, 100 mM non-essential amino acids, 0.1 mM β-mercaptoethanol, 1 mM sodium pyruvate (Invitrogen) and 1,000 U/mL LIF (Millipore) on gelatin-coated plates. MEF and HEK293T cells were cultured in DMEM supplemented with 10% FBS (Invitrogen).

Stat3 shRNA was cloned into pLVX vector with target sequence of GATCCCCGGGCCATCCTAAGCACAAAttcaagagaTTTGTGCTT AGGATGGCCCTTTTTA and co-transfected into HEK293T cells with pVSVG and gag/pol plasmids. Twelve hours after transfection, cells were cultured with DMEM medium containing 20% FBS for an additional 24 hr. The culture medium containing lentivirus particles was filtered through a 0.45-μm filter (Millipore) and incubated with mESCs supplemented with 4 mg/mL polybrene (Sigma) for 12 hr, followed by selection with 5 mg/mL puromycin for another 24 hr.

AP Staining

AP staining was detected using the Alkaline Phosphatase Detection Kit (Millipore) according to the manufacturer's recommendations.

RNA Extraction, Reverse Transcription, and Quantitative Real-Time PCR

RNA was extracted using TRIzol reagent (Invitrogen) and treated with DNaseI (Amicon). cDNA synthesis was performed with 1 μg of total RNA and the Superscript III kit (Invitrogen) according to the manufacturer's instructions. Endogenous mRNA levels were measured by real-time PCR analysis based on SYBR Green detection with an ABI real-time PCR machine. The sequence of real-time PCR primers is provided in Table S4. Samples were assayed in duplicate and normalized to endogenous *actin*.

Microarray Analysis

mESCs were transfected with siRNA targeted against either *Mettl8* or a scrambled siRNA control. After 72 hr growth in selection media, total RNA was isolated by an RNAeasy purification kit (QIAGEN). Microarray analysis was performed using an Agilent whole-mouse gene expression microarray according to the manufacturer's instructions. Duplicate samples were used to compare transcript expression differences between *Mettl8*-siRNA and scrambled-siRNA ESCs.

Protein Extraction and Western Blot

Protein extracts were obtained using cell lysis buffer (20 mM HEPES, 400 nM NaCl, 0.5% NP-40, 10% glycerol, 1 mM DTT) with protease inhibitor (Roche) and phosphatase inhibitor. Proteins were separated by SDS-PAGE, transferred to polyvinylidene fluoride membrane (Bio-Rad), and probed with specific primary antibody and appropriate HRP-conjugated secondary antibody. Signals were detected using SuperSignal West Pico Chemiluminescent Substrate (Pierce). The following antibodies were used for western blot: α-STAT3 (1:1,000, Santa Cruz, sc-482), p-STAT3Y705 (1:1,000, Cell Signaling Technology, no. 9131), METTL8 polyclonal (1:2,000, produced by our lab), METTL8 monoclonal (1:1,000, produced by our lab), α-tubulin (1:2,500, Santa Cruz, sc-53646), β-actin (1:2,500, Santa Cruz, sc-8432), SOCS3 (1:1,000, Cell Signaling, no. 2923), OCT4 (1:1,000, Cell Signaling, no. 2840), SOX2 (1:200, Santa Cruz, sc-365964), MAPKBP1 (1:200, Santa Cruz, sc-514754), and Flag (1:1,000, Sigma, F1804).

ChIP

ChIP assays with mESCs were carried out as described previously (Loh et al., 2006). In brief, cells were crosslinked with 1% formaldehyde for 10 min at room temperature and formaldehyde was neutralized by addition of 0.2 M glycine. Chromatin extracts containing DNA fragments with an average size of 500 bp were immunoprecipitated using α-pY705-STAT3 antibody. For all ChIP experiments, quantitative real-time PCR analyses were performed using SYBR-Green Master Mix.

RIP

RIP was performed as described previously (McHugh et al., 2015). In brief, $1-3 \times 10^7$ cells were lysed in hypotonic buffer supplemented with RNase A inhibitor and DNase I before centrifugation. Cell lysates were precleared with protein A/G beads (Pierce) before they were incubated with protein A/G beads coated with the indicated antibodies at 4°C for 3 hr. After extensive washing, the

bead-bound immunocomplexes were eluted using elution buffer (50 mM Tris [pH 8.0], 1% SDS, and 10 mM EDTA) at 65°C for 10 min. To isolate protein-associated RNAs from the eluted immunocomplexes, samples were treated with proteinase K, and RNAs were extracted by phenol/chloroform. Purified RNAs were then subjected to real-time PCR analysis.

Biotin Pull-Down Assay

All processes were performed in the RNase-free conditions. For anti-sense oligomer affinity pull-down assay, sense or antisense biotin-labeled DNA oligomers corresponding to *Mapkbp1* mRNA (3 mg) were incubated with lysates from 2 to $3 \times 10^7 \times 10^{14}$ cells. One hour after incubation, streptavidin-coupled Dynabeads (Invitrogen) were added to isolate the RNA-protein complex. For in vitro RNA pull-down assay, 3 mg in-vitro-synthesized biotin-labeled *Mapkbp1* mRNA was incubated with purified flag or flag-METTL8 protein for 3 hr. Streptavidin-coupled Dynabeads (Invitrogen) were then added to the reaction mix to isolate the RNA-protein complex.

Polysome Analysis

E14 cells were preincubated with CHX (100 μg/mL, Sigma) for 15 min, and cytoplasmic lysates were prepared and fractionated by ultracentrifugation through 15%–50% linear sucrose gradients; 15 fractions were collected, and RNA extracted from each fraction was used for quantitative real-time PCR analysis.

CRISPR KO in E14 Cells

E14 cells were transfected with pX459 plasmids containing gRNAs for *Mettl8* or *Mapkbp1*. Forty-eight hours later cells were treated with puromycin (5 μg/mL) for 48 hr. Then the live cells were collected, and each single cell was re-plated into 96-well plates and cultured. The knockout efficiency was confirmed by western blot.

Colony-Forming Assay

Colony-forming assay was performed as described previously (Gu et al., 2015). In brief, ESCs were trypsinized to obtain a single-cell suspension, and 600 cells were plated per 10-cm^2 well. After 6 days, colonies were stained for AP activity and divided into two categories: differentiated and undifferentiated.

JNK Assay

Cell lysates were incubated with c-Jun-conjugated beads and JNK activity was analyzed using a JNK activity assay kit (New England Bio Labs) according to manufacturer's instructions.

Neuron Progenitor Cell Differentiation

Neuron progenitor cell differentiation assay was performed as described previously (Lau et al., 2006). To produce EBs, 200×10^{14} cells were cultured in hanging drops for 3 days. Ten EBs were plated on gelatin-coated dishes in knockout DMEM containing epidermal growth factor, basic fibroblast growth factor, and L-ascorbic acid. Eight to 24 hr later, the medium was replaced by proliferation medium: DMEM/F12 supplemented with 10% FBS, 2 mM L-glutamine, 20 nM progesterone, 100 mM putrescine, 25 mg/mL insulin, 50 mg/mL transferrin, and 30 nM sodium selenite.

Cardiac Differentiation

Cardiac differentiation assay was performed as described previously (Boheler, 2002). E14 cells were culture in hanging drops with differentiation media (DMEM supplemented with 10% FBS, L-glutamine, non-essential amino acids, sodium pyruvate, penicillin-streptomycin, β-mercaptoethanol, and ascorbic acid) (50 mg/mL), and diluted to 1,000 cells per 25 μL for 3 days. At day 4, EBs were transferred into gelatin-coated dishes, and the beating cardiomyocytes could be observed as early as day 8.

Induced Pluripotent Stem Cells

Animals were maintained in a certified facility, and all protocols were approved by IACUC of National University of Singapore. All procedures related to animals were performed in accordance with guidelines of AAALAC. iPSCs were induced as described previously (Carey et al., 2010). MEF cells were isolated from E13.5 embryos of $Gt(ROSA)26Sor^{tm1(rtTA*M2)Jae}$ $Col1a1^{tm3(tetO-Pou5f1,-Sox2,-Klf4,-Myc)Jae}$/ J mice. Cells were treated with doxycycline and 20 days later iPSC colonies were counted.

ACCESSION NUMBERS

The accession number for the RNA-seq reported in this paper is GEO: GSE112360.

SUPPLEMENTAL INFORMATION

Supplemental Information includes seven figures and four tables and can be found with this article online at https://doi.org/10.1016/j.stemcr.2018.03.022.

AUTHOR CONTRIBUTIONS

H.G. and X.-Y.F. conceived and designed the project. H.G., D.V.D., and X.L. performed most of the experiments and analyzed the data. L.X. helped on *Mettl8* KO ESC, RIP, and translational study. Y.S. performed FACS analysis. Y.W. helped with cardiomyocytes differentiation. N.S. helped to create the *Mettl8* KO mice under J.Y.'s and X.L.'s guidance. Y.L. and H.Y. analyzed the RNA-seq data. G.A.T. provided technical assistance. J.M.N. and H.G. performed the sucrose gradient sedimentation. H.G., X.L., and X.F. wrote the manuscript. All authors discussed the results and commented on the manuscript.

ACKNOWLEDGMENTS

REFERENCES

Akira, S., Nishio, Y., Inoue, M., Wang, X.J., Wei, S., Matsusaka, T., Yoshida, K., Sudo, T., Naruto, M., and Kishimoto, T. (1994). Molecular cloning of APRF, a novel IFN-stimulated gene factor 3 p91-related transcription factor involved in the gp130-mediated signaling pathway. Cell 77, 63–71.

Boeuf, H., Hauss, C., Graeve, F.D., Baran, N., and Kedinger, C. (1997). Leukemia inhibitory factor-dependent transcriptional activation in embryonic stem cells. J. Cell Biol. 138, 1207–1217.

Boheler, K.R. (2002). Differentiation of pluripotent embryonic stem cells into cardiomyocytes. Circ. Res. 91, 189–201.

Boyer, L.A., Lee, T.I., Cole, M.F., Johnstone, S.E., Levine, S.S., Zucker, J.P., Guenther, M.G., Kumar, R.M., Murray, H.L., Jenner, R.G., et al. (2005). Core transcriptional regulatory circuitry in human embryonic stem cells. Cell 122, 947–956.

Carey, B.W., Markoulaki, S., Beard, C., Hanna, J., and Jaenisch, R. (2010). Single-gene transgenic mouse strains for reprogramming adult somatic cells. Nat. Methods 7, 56–59.

Chen, X., Xu, H., Yuan, P., Fang, F., Huss, M., Vega, V.B., Wong, E., Orlov, Y.L., Zhang, W., Jiang, J., et al. (2008). Integration of external signaling pathways with the core transcriptional network in embryonic stem cells. Cell 133, 1106–1117.

Cui, Q., Shi, H., Ye, P., Li, L., Qu, Q., Sun, G., Sun, G., Lu, Z., Huang, Y., and Yang, C.-G. (2017). m6A RNA methylation regulates the self-renewal and tumorigenesis of glioblastoma stem cells. Cell Rep. 18, 2622–2634.

Darnell, J.E., Jr., Kerr, I.M., and Stark, G.R. (1994). Jak-STAT pathways and transcriptional activation in response to IFNs and other extracellular signaling proteins. Science 264, 1415–1421.

Davis, R.J. (2000). Signal transduction by the JNK group of MAP kinases. Cell 103, 239–252.

Dérijard, B., Hibi, M., Wu, I.-H., Barrett, T., Su, B., Deng, T., Karin, M., and Davis, R.J. (1994). JNK1: a protein kinase stimulated by UV light and Ha-Ras that binds and phosphorylates the c-Jun activation domain. Cell 76, 1025–1037.

Do, D.V., Ueda, J., Messerschmidt, D.M., Lorthongpanich, C., Zhou, Y., Feng, B., Guo, G., Lin, P.J., Hossain, M.Z., Zhang, W., et al. (2013). A genetic and developmental pathway from STAT3 to the OCT4-NANOG circuit is essential for maintenance of ICM lineages in vivo. Genes Dev. 27, 1378–1390.

Fu, X.Y., Kessler, D.S., Veals, S.A., Levy, D.E., and Darnell, J.E., Jr. (1990). ISGF3, the transcriptional activator induced by interferon alpha, consists of multiple interacting polypeptide chains. Proc. Natl. Acad. Sci. USA. 87, 8555–8559.

Fu, X.Y., Schindler, C., Improta, T., Aebersold, R., and Darnell, J.E., Jr. (1992). The proteins of ISGF-3, the interferon alpha-induced transcriptional activator, define a gene family involved in signal transduction. Proc. Natl. Acad. Sci. USA. 89, 7840–7843.

Geula, S., Moshitch-Moshkovitz, S., Dominissini, D., Mansour, A.A., Kol, N., Salmon-Divon, M., Hershkovitz, V., Peer, E., Mor, N., and Manor, Y.S. (2015). m6A mRNA methylation facilitates resolution of naïve pluripotency toward differentiation. Science 347, 1002–1006.

Gu, H., Li, Q., Huang, S., Lu, W., Cheng, F., Gao, P., Wang, C., Miao, L., Mei, Y., and Wu, M. (2015). Mitochondrial E3 ligase March5 maintains stemness of mouse ESCs via suppression of ERK signalling. Nat. Commun. 6, 7112.

Hafner, M., Landthaler, M., Burger, L., Khorshid, M., Hausser, J., Berninger, P., Rothballer, A., Ascano, M., Jr., Jungkamp, A.C., Munschauer, M., et al. (2010). Transcriptome-wide identification of RNA-binding protein and microRNA target sites by PAR-CLIP. Cell 141, 129–141.

Hibi, M., Lin, A., Smeal, T., Minden, A., and Karin, M. (1993). Identification of an oncoprotein-and UV-responsive protein kinase that binds and potentiates the c-Jun activation domain. Genes Dev. 7, 2135–2148.

Jaeschke, A., Karasarides, M., Ventura, J.J., Ehrhardt, A., Zhang, C., Flavell, R.A., Shokat, K.M., and Davis, R.J. (2006). JNK2 is a positive regulator of the cJun transcription factor. Mol. Cell 23, 899–911.

Koyano, S., Ito, M., Takamatsu, N., Shiba, T., Yamamoto, K.-i., and Yoshioka, K. (1999). A novel Jun N-terminal kinase (JNK)-binding protein that enhances the activation of JNK by MEK kinase 1 and TGF-β-activated kinase 1. FEBS Lett. 457, 385–388.

Lau, T., Adam, S., and Schloss, P. (2006). Rapid and efficient differentiation of dopaminergic neurons from mouse embryonic stem cells. Neuroreport 17, 975–979.

Lecat, A., Di Valentin, E., Somja, J., Jourdan, S., Fillet, M., Kufer, T.A., Habraken, Y., Sadzot, C., Louis, E., Delvenne, P., et al. (2012). The c-Jun N-terminal kinase (JNK)-binding protein (JNKBP1) acts as a negative regulator of NOD2 protein signaling by inhibiting its oligomerization process. J. Biol. Chem. 287, 29213–29226.

Lim, C.P., and Cao, X. (1999). Serine phosphorylation and negative regulation of Stat3 by JNK. J. Biol. Chem. 274, 31055–31061.

Liu, J., Yue, Y., Han, D., Wang, X., Fu, Y., Zhang, L., Jia, G., Yu, M., Lu, Z., and Deng, X. (2014). A METTL3-METTL14 complex mediates mammalian nuclear RNA N6-adenosine methylation. Nat. Chem. Biol. 10, 93–95.

Loh, Y.H., Wu, Q., Chew, J.L., Vega, V.B., Zhang, W., Chen, X., Bourque, G., George, J., Leong, B., Liu, J., et al. (2006). The Oct4 and Nanog transcription network regulates pluripotency in mouse embryonic stem cells. Nat. Genet. 38, 431–440.

McHugh, C.A., Chen, C.-K., Chow, A., Surka, C.F., Tran, C., McDonel, P., Pandya-Jones, A., Blanco, M., Burghard, C., and Moradian, A. (2015). The Xist lncRNA interacts directly with SHARP to silence transcription through HDAC3. Nature 521, 232–236.

Niwa, H., Burdon, T., Chambers, I., and Smith, A. (1998). Self-renewal of pluripotent embryonic stem cells is mediated via activation of STAT3. Genes Dev. 12, 2048–2060.

Raz, R., Lee, C.K., Cannizzaro, L.A., d'Eustachio, P., and Levy, D.E. (1999). Essential role of STAT3 for embryonic stem cell pluripotency. Proc. Natl. Acad. Sci. USA. 96, 2846–2851.

Sabapathy, K., Hochedlinger, K., Nam, S.Y., Bauer, A., Karin, M., and Wagner, E.F. (2004). Distinct roles for JNK1 and JNK2 in regulating JNK activity and c-Jun-dependent cell proliferation. Mol. Cell 15, 713–725.
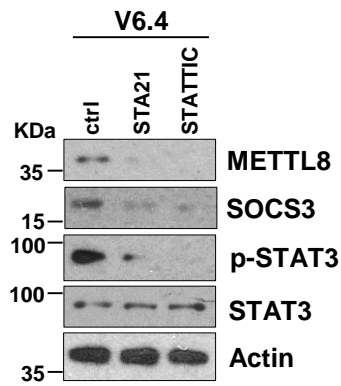
Schindler, C., Shuai, K., Prezioso, V.R., and Darnell, J.E., Jr. (1992). Interferon-dependent tyrosine phosphorylation of a latent cytoplasmic transcription factor. Science *257*, 809–813.

Schust, J., Sperl, B., Hollis, A., Mayer, T.U., and Berg, T. (2006). Stattic: a small-molecule inhibitor of STAT3 activation and dimerization. Chem. Biol. *13*, 1235–1242.

Smith, A.G., Heath, J.K., Donaldson, D.D., Wong, G.G., Moreau, J., Stahl, M., and Rogers, D. (1988). Inhibition of pluripotential embryonic stem cell differentiation by purified polypeptides. Nature *336*, 688–690.

Song, H., Wang, R., Wang, S., and Lin, J. (2005). A low-molecular-weight compound discovered through virtual database screening inhibits Stat3 function in breast cancer cells. Proc. Natl. Acad. Sci. USA. *102*, 4700–4705.

Takeda, K., Noguchi, K., Shi, W., Tanaka, T., Matsumoto, M., Yoshida, N., Kishimoto, T., and Akira, S. (1997). Targeted disruption of the mouse Stat3 gene leads to early embryonic lethality. Proc. Natl. Acad. Sci. USA. *94*, 3801–3804.

Tiwari, V.K., Stadler, M.B., Wirbelauer, C., Paro, R., Schubeler, D., and Beisel, C. (2011). A chromatin-modifying function of JNK during stem cell differentiation. Nat. Genet. *44*, 94–100.

Weston, C.R., and Davis, R.J. (2007). The JNK signal transduction pathway. Curr. Opin. Cell Biol. *19*, 142–149.

Williams, R.L., Hilton, D.J., Pease, S., Willson, T.A., Stewart, C.L., Gearing, D.P., Wagner, E.F., Metcalf, D., Nicola, N.A., and Gough, N.M. (1988a). Myeloid leukaemia inhibitory factor maintains the developmental potential of embryonic stem cells. Nature *336*, 684–687.

Williams, R.L., Hiltonl, D.J., and Nicolai, N.A. (1988b). Potential of embryonic stem cells. Nature *336*, 15.

Xu, L., Liu, X., Sheng, N., Oo, K.S., Liang, J., Chionh, Y.H., Xu, J., Ye, F., Gao, Y.-G., and Dedon, P.C. (2017). Three distinct 3-methylcytidine (m3C) methyltransferases modify tRNA and mRNA in mice and humans. J. Biol. Chem. *292*, 14695–14703.

Xu, P., and Davis, R.J. (2010). c-Jun NH2-terminal kinase is required for lineage-specific differentiation but not stem cell self-renewal. Mol. Cell Biol. *30*, 1329–1340.

Ying, Q.L., Nichols, J., Chambers, I., and Smith, A. (2003). BMP induction of Id proteins suppresses differentiation and sustains embryonic stem cell self-renewal in collaboration with STAT3. Cell *115*, 281–292.

Zhong, Z., Wen, Z., and Darnell, J.E., Jr. (1994). Stat3: a STAT family member activated by tyrosine phosphorylation in response to epidermal growth factor and interleukin-6. Science *264*, 95–98.

Supplemental Information

The STAT3 Target *Mettl8* Regulates Mouse ESC Differentiation via Inhibiting the JNK Pathway
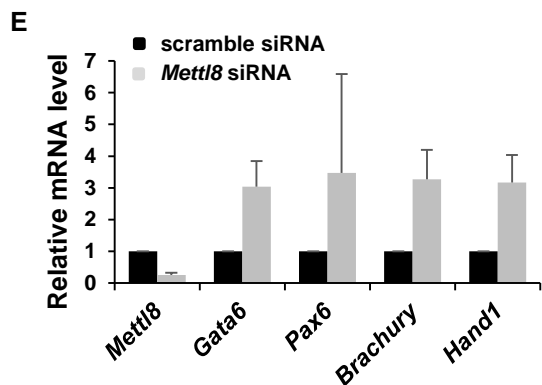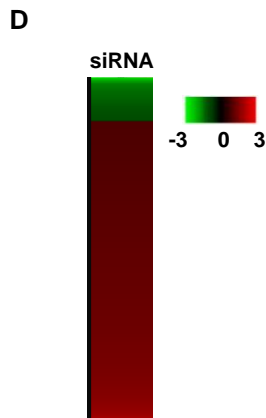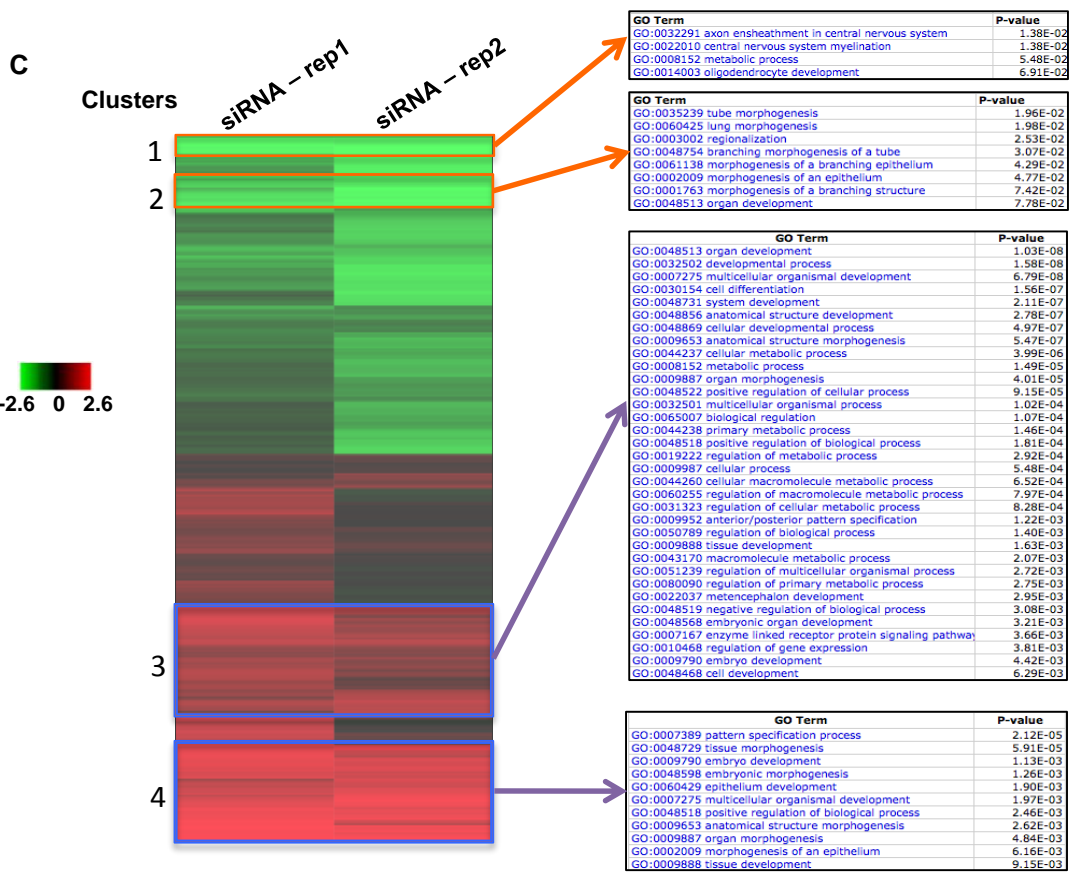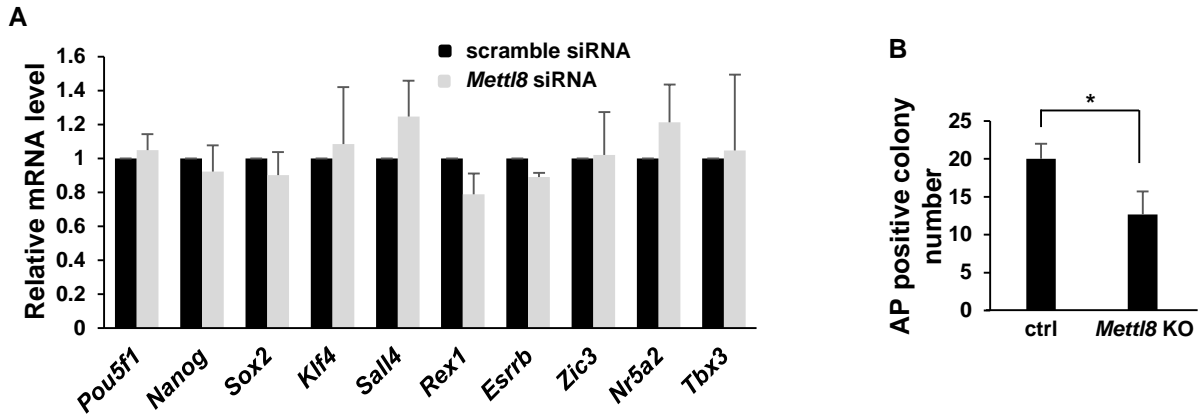
Hao Gu, Dang Vinh Do, Xinyu Liu, Luang Xu, Yixun Su, Jie Min Nah, Yuqian Wong, Ying Li, Na Sheng, Gebreselassie Addisu Tilaye, Henry Yang, Huili Guo, Jun Yan, and Xin-Yuan Fu

Figure S1. *Mettl8* **is transcriptionally regulated by STAT3. Related to Figure 1.**

V6.4 cells were treated with STA-21 and STATTIC for 6 hours and harvested. Then cell lysates were analysed by western blot.
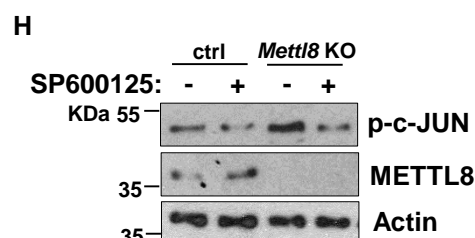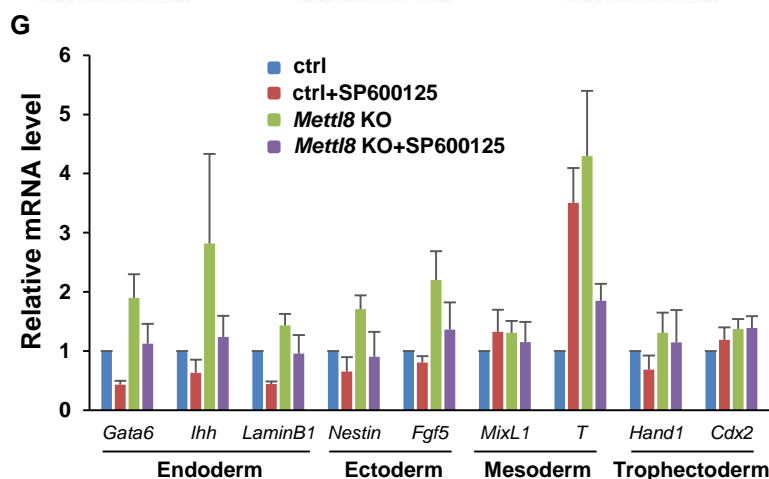
A

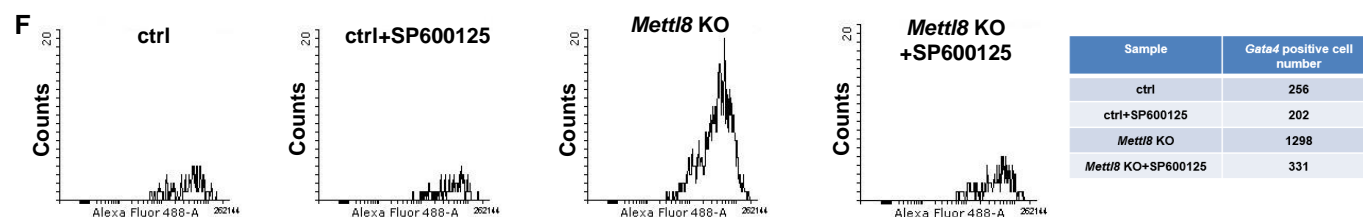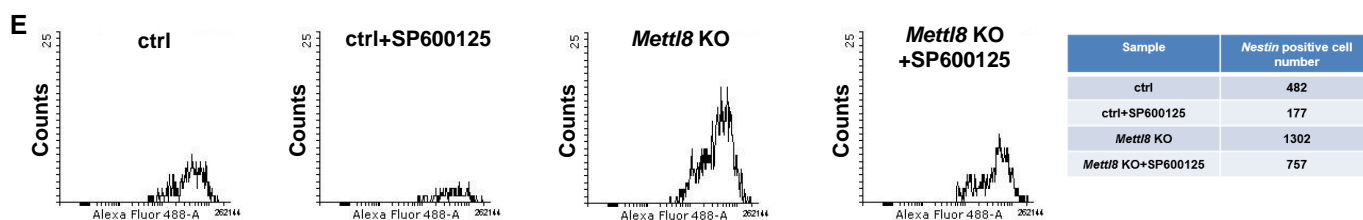Relative mRNA level (Pou5f1, Nanog, Sox2, Klf4, Sall4, Rex1, Esrrb, Zic3, Nr5a2, Tbx3)
- scramble siRNA
- Mettl8 siRNA

B

AP positive colony number (ctrl, Mettl8 KO)
*

C

Clusters (siRNA – rep1, siRNA – rep2): 1, 2, 3, 4

GO Term	P-value
GO:0032291 axon ensheathment in central nervous system	1.38E-02
GO:0022010 central nervous system myelination	1.38E-02
GO:0008152 metabolic process	5.48E-02
GO:0014003 oligodendrocyte development	6.91E-02

GO Term	P-value
GO:0035239 tube morphogenesis	1.96E-02
GO:0060425 lung morphogenesis	1.98E-02
GO:0003002 regionalization	2.53E-02
GO:0048754 branching morphogenesis of a tube	3.07E-02
GO:0061138 morphogenesis of a branching epithelium	4.29E-02
GO:0002009 morphogenesis of an epithelium	4.77E-02
GO:0001763 morphogenesis of a branching structure	7.42E-02
GO:0048513 organ development	7.78E-02

GO Term	P-value
GO:0048513 organ development	1.03E-08
GO:0032502 developmental process	1.58E-08
GO:0007275 multicellular organismal development	6.79E-08
GO:0030154 cell differentiation	1.56E-07
GO:0048731 system development	2.11E-07
GO:0048856 anatomical structure development	2.78E-07
GO:0048869 cellular developmental process	4.97E-07
GO:0009653 anatomical structure morphogenesis	5.47E-07
GO:0044237 cellular metabolic process	3.99E-06
GO:0008152 metabolic process	1.49E-05
GO:0009887 organ morphogenesis	4.01E-05
GO:0048522 positive regulation of cellular process	9.15E-05
GO:0032501 multicellular organismal process	1.02E-04
GO:0065007 biological regulation	1.07E-04
GO:0044238 primary metabolic process	1.46E-04
GO:0048518 positive regulation of biological process	1.81E-04
GO:0019222 regulation of metabolic process	2.92E-04
GO:0009987 cellular process	5.48E-04
GO:0044260 cellular macromolecule metabolic process	6.52E-04
GO:0060255 regulation of macromolecule metabolic process	7.97E-04
GO:0031323 regulation of cellular metabolic process	8.28E-04
GO:0009952 anterior/posterior pattern specification	1.22E-03
GO:0050789 regulation of biological process	1.40E-03
GO:0009888 tissue development	1.63E-03
GO:0043170 macromolecule metabolic process	2.07E-03
GO:0051239 regulation of multicellular organismal process	2.72E-03
GO:0080090 regulation of primary metabolic process	2.75E-03
GO:0022037 metencephalon development	2.95E-03
GO:0048519 negative regulation of biological process	3.08E-03
GO:0048568 embryonic organ development	3.21E-03
GO:0007167 enzyme linked receptor protein signaling pathway	3.66E-03
GO:0010468 regulation of gene expression	3.81E-03
GO:0009790 embryo development	4.42E-03
GO:0048468 cell development	6.29E-03

GO Term	P-value
GO:0007389 pattern specification process	2.12E-05
GO:0048729 tissue morphogenesis	5.91E-05
GO:0009790 embryo development	1.13E-03
GO:0048598 embryonic morphogenesis	1.26E-03
GO:0060429 epithelium development	1.90E-03
GO:0007275 multicellular organismal development	1.97E-03
GO:0048518 positive regulation of biological process	2.46E-03
GO:0009653 anatomical structure morphogenesis	2.62E-03
GO:0009887 organ morphogenesis	4.84E-03
GO:0002009 morphogenesis of an epithelium	6.16E-03
GO:0009888 tissue development	9.15E-03

D

siRNA

E

Relative mRNA level (Mettl8, Gata6, Pax6, Brachury, Hand1)
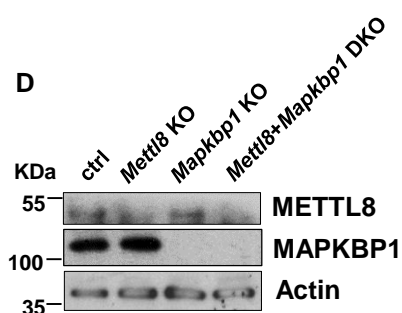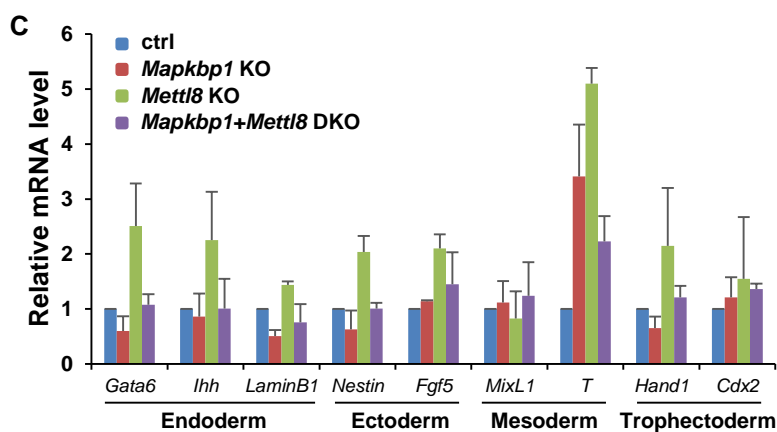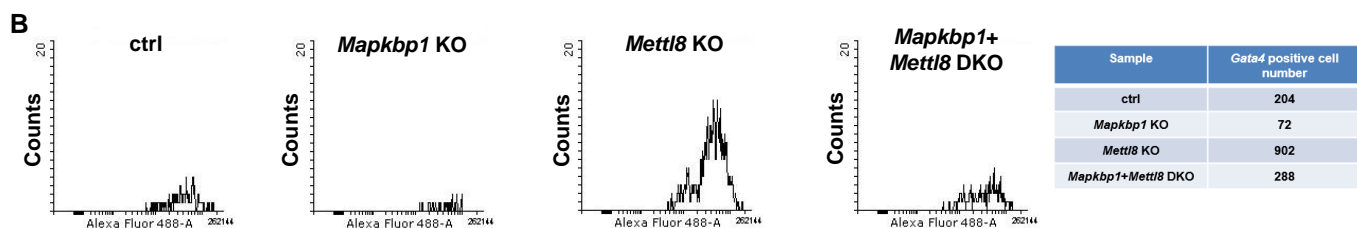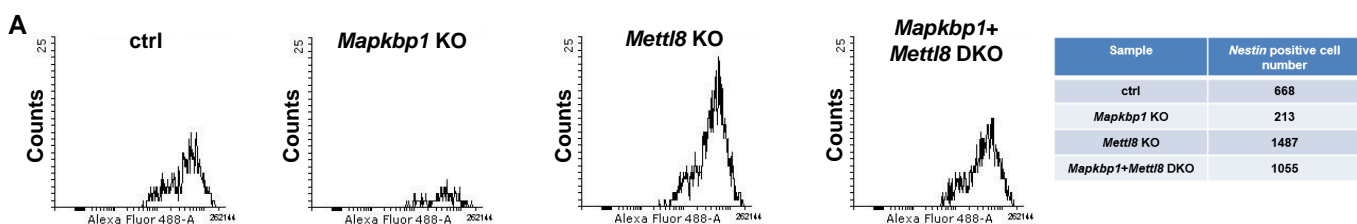- scramble siRNA
- Mettl8 siRNA

Figure S2. METTL8 affects ESCs differentiation rather than pluripotency. Related to Figure 2.

(A) Quantitative RT-PCR analysis showed no significant change in expression of the key pluripotent genes.

(B) *Mettl8* KO and control V6.4 cells were subjected to EB formation for 7 days. EBs were trypsinized and re-plated into gelatin-coated dished. After 3 days culture in ES medium, colonies were stained for AP activity and AP positive colonies were counted. Data are shown as the mean$\pm$s.d. from 3 independent experiments.* means P<0.05.

(C) Microarray profiling of gene expression changes in ES cells after knocking down *Mettl8* and Log$_2$ transformed fold gene expression differences. siRNA-rep 1 and siRNA-rep 2 represents two independent comparisons of transcriptomes of mES cells treated with *Mettl8* siRNA compared to those treated with scramble siRNA control in two independent experiments.

(D) RNA-seq analysis of gene expression changes in ES cells after knocking down *Mettl8.* Log$_2$ transformed fold gene expression differences were subject to hierarchical clustering.

(E) Five upregulated developmental genes from microarray and RNA-seq results are selected for validation by realtime-PCR. The transcript levels of all genes were normalized to *Gapdh* expression level.
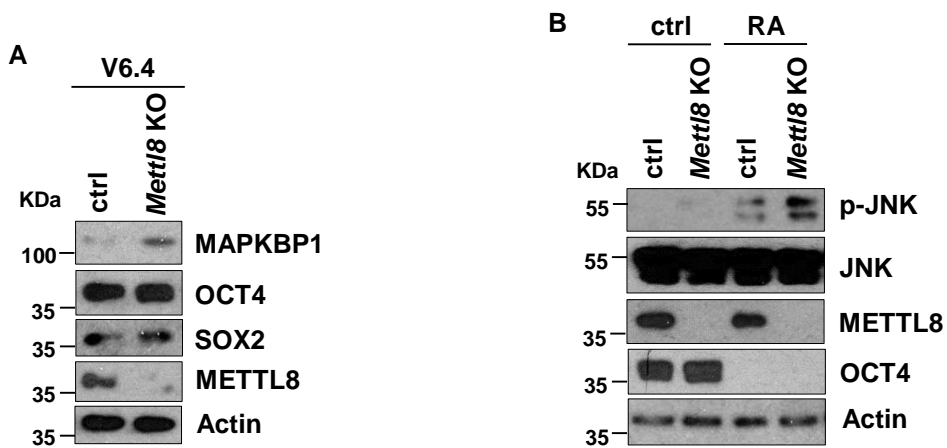
Figure S3. METTL8 inhibits JNK signaling in V6.4 mESCs. Related to Figure 6.

(A) Cell lysates of *Mettl8* KO and control V6.4 cells were analysed by western blot.

(B) *Mettl8* KO and control V6.4 cells were treated with RA for 6 days and cell lysates were analysed by western blot.

A

ctrl   *Mapkbp1* KO   *Mettl8* KO   *Mapkbp1+ Mettl8* DKO

Sample	*Nestin* positive cell number
ctrl	668
Mapkbp1 KO	213
Mettl8 KO	1487
Mapkbp1+Mettl8 DKO	1055

B

ctrl   *Mapkbp1* KO   *Mettl8* KO   *Mapkbp1+ Mettl8* DKO

Sample	*Gata4* positive cell number
ctrl	204
Mapkbp1 KO	72
Mettl8 KO	902
Mapkbp1+Mettl8 DKO	288

C

- ctrl
- *Mapkbp1* KO
- *Mettl8* KO
- *Mapkbp1+Mettl8* DKO

Endoderm: *Gata6*, *Ihh*, *LaminB1* — Ectoderm: *Nestin*, *Fgf5* — Mesoderm: *MixL1*, *T* — Trophectoderm: *Hand1*, *Cdx2*

D

KDa: 55, 100, 35 — METTL8, MAPKBP1, Actin

ctrl, *Mettl8* KO, *Mapkbp1* KO, *Mettl8+Mapkbp1* DKO

E

ctrl   ctrl+SP600125   *Mettl8* KO   *Mettl8* KO +SP600125

Sample	*Nestin* positive cell number
ctrl	482
ctrl+SP600125	177
Mettl8 KO	1302
Mettl8 KO+SP600125	757

F

ctrl   ctrl+SP600125   *Mettl8* KO   *Mettl8* KO +SP600125

Sample	*Gata4* positive cell number
ctrl	256
ctrl+SP600125	202
Mettl8 KO	1298
Mettl8 KO+SP600125	331

G

- ctrl
- ctrl+SP600125
- *Mettl8* KO
- *Mettl8* KO+SP600125

Endoderm: *Gata6*, *Ihh*, *LaminB1* — Ectoderm: *Nestin*, *Fgf5* — Mesoderm: *MixL1*, *T* — Trophectoderm: *Hand1*, *Cdx2*

H

ctrl, *Mettl8* KO — SP600125: - + - +

KDa: 55, 35, 35 — p-c-JUN, METTL8, Actin

Figure S4. The METTL8-JNK pathway in ESCs differentiation. Related to Figure 7.

(A) Re-confirm the number of Nestin positive cells by FACS. *Mettl8* KO, *Mapkbp1* KO, *Mettl8* and *Mapkbp1* DKO and control E14 cells were subjected to neuron progenitor cells differentiation. Cells were stained for expression of Nestin and half of cells from one 12-well plate were analysed by FACS.

(B) Re-confirm the number of Gata4 positive cells by FACS. Mettl8 KO, *Mapkbp1* KO, *Mettl8* and *Mapkbp1* DKO and control E14 cells were subjected to cardiac differentiation. Cells were stained for expression of Gata4 and 10% cells from one 12-well plate were analysed by FACS.

(C-D) *Mettl8* KO, *Mapkbp1* KO, *Mettl8* and *Mapkbp1* DKO and control E14 cells were subjected to EB formation. Fourteen days later, (C) total RNAs were extracted and RNA levels of lineage markers were analysed by RT-PCR. Data are shown as the mean±s.d. from 3 independent experiments. (D) Cell lysates were analysed by western blot.

(E) Re-confirm the number of Nestin positive cells by FACS. *Mettl8* KO and control E14 cells were treated with or without SP600125 and subjected to neuron progenitor cells differentiation. Cells were stained for expression of Nestin and half of cells from one 12-well plate were analysed by FACS.

(F) Re-confirm the number of Gata4 positive cells by FACS. *Mettl8* KO and control E14 cells were treated with or without SP600125 and subjected to cardiac differentiation. Cells were stained for expression of Gata4 and 10% cells from one 12-well plate were analysed by FACS.

(G-H) *Mettl8* KO and control E14 cells were treated with or without SP600125 and subjected to EB formation. Fourteen days later, (G) total RNAs were extracted and RNA levels of lineage markers were analysed by RT-PCR. Data are shown as the mean±s.d. from 3 independent experiments. (H) Cell lysates were analysed by western blot.
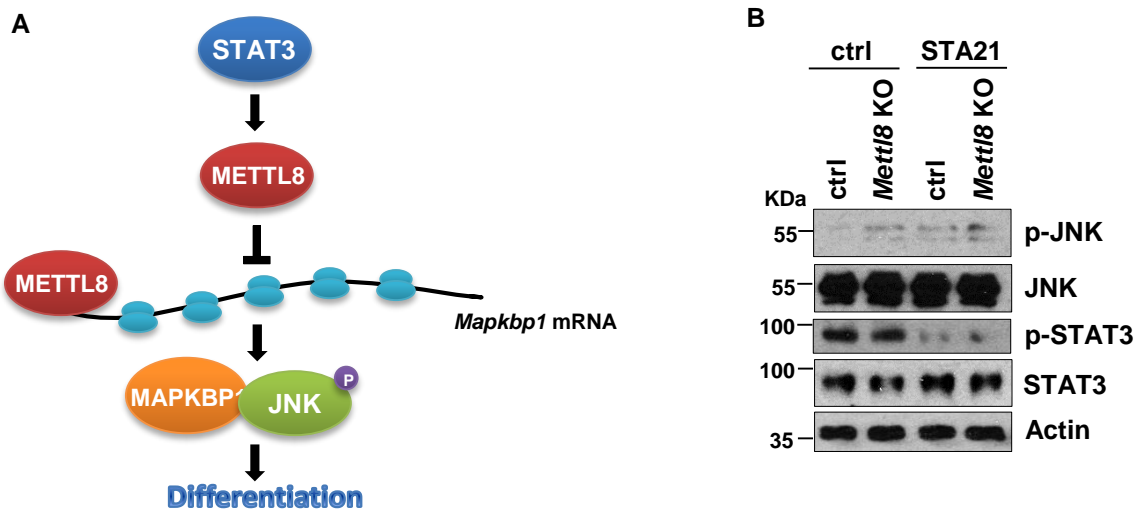
Figure S5. The STAT3-METTL8-JNK pathway in mouse ESCs

(A) A proposed model illustrating the role of the STAT3-METTL8-MAPKBP1-JNK pathway in mouse ESCs.

(B) Control and *Mettl8* KO E14 cells were treated RA for 4 days. Then cells were treated with or without STA21 for 12 hours and cell lysates were analysed by western blot.
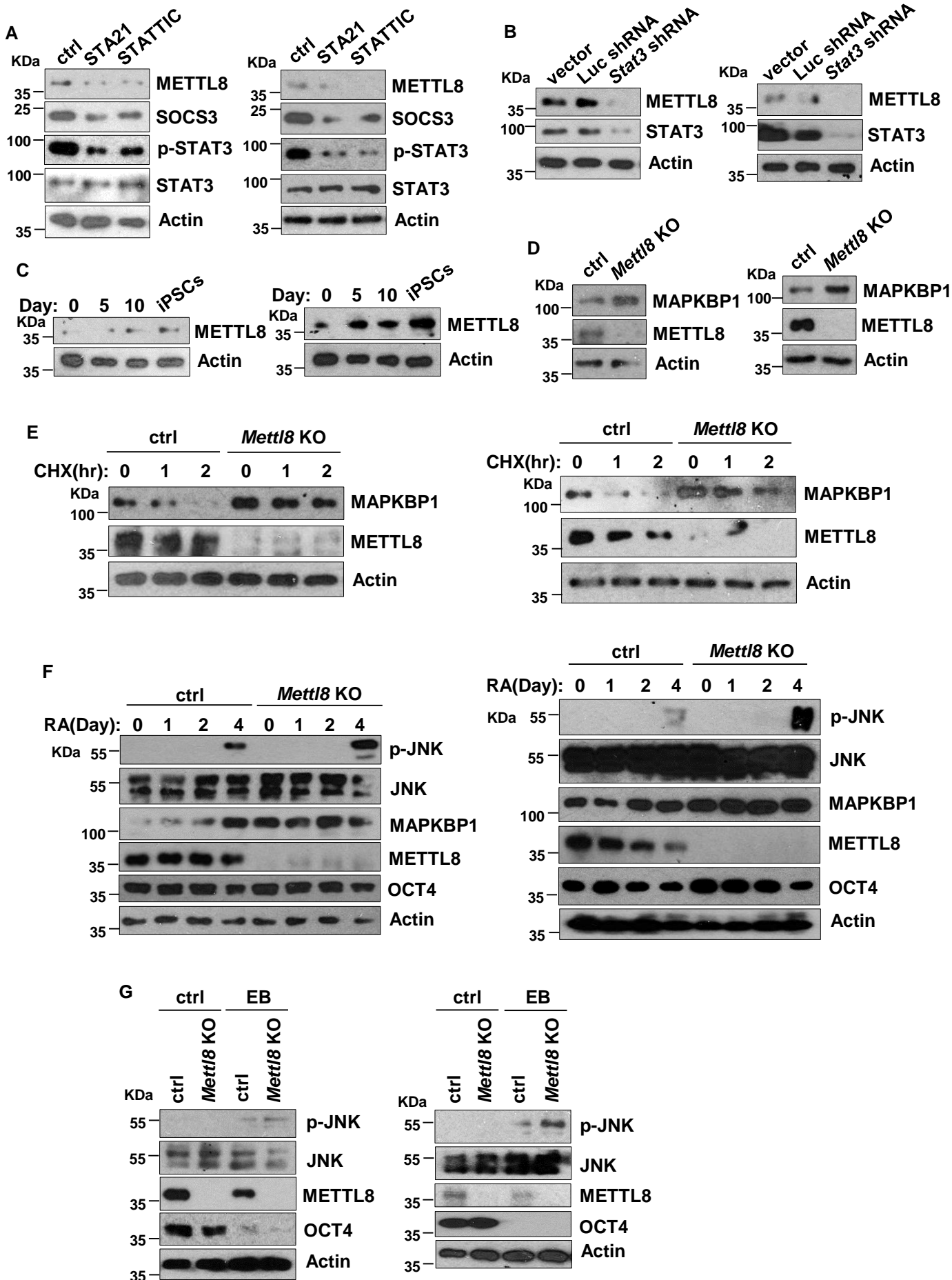
Figure S6. Replicates of western blot quantifications

(A)   Replicates of Fig.1C

(B)   Replicates of Fig.1E

(C)   Replicates of Fig.3B

(D)   Replicates of Fig.5C

(E)   Replicates of Fig.5D

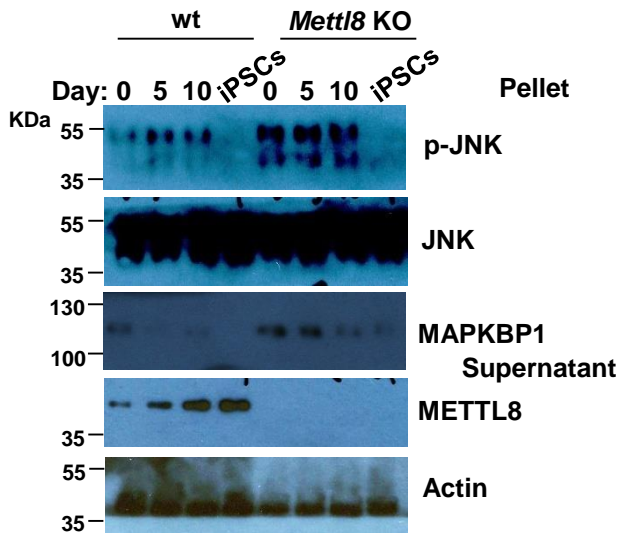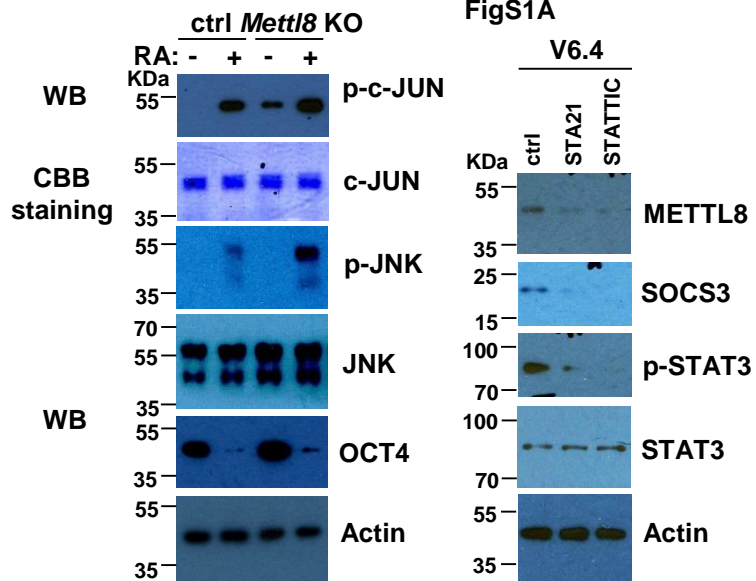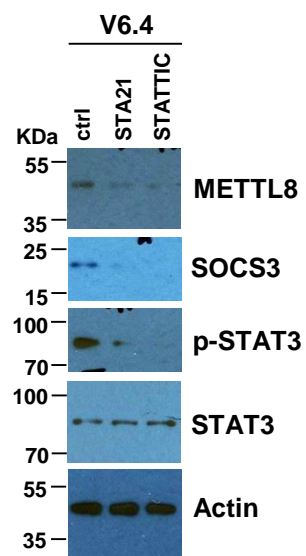(F)   Replicates of Fig.6B

(G)   Replicates of Fig.6C

Fig1C

KDa | ctrl | STA21 | STATTIC
55 / 35 — METTL8
25 / 15 — SOCS3
100 / 70 — p-STAT3
100 / 70 — STAT3
35 — Actin

Fig1E

KDa | vector | Luc shRNA | Stat3 shRNA
55 / 35 — METTL8
100 / 70 — STAT3
55 / 35 — Actin

Fig1G

Flag-STAT3 : - + ++
KDa
55 / 35 — METTL8
100 / 70 — Flag-STAT3
35 — Actin

Fig1I

LIF: - + - +
Dox : - - + +
KDa
100 / 70 — p-STAT3
100 / 70 — STAT3
55 / 35 — Flag-METTL8
35 — Actin

Fig2B

RA(Day): 0 1 2 4
KDa
55 / 35 — METTL8
100 / 70 — STAT3
100 / 70 — p-STAT3
55 / 35 — OCT4
55 / 35 — Actin

Fig2D

EB(Day): 0 3 6 9 15
KDa
55 / 35 — METTL8
55 / 35 — OCT4
35 — Actin

Fig2G

KDa | ctrl | Mettl8 KO
OCT4
SOX2
METTL8
Tubulin

Fig2H

KDa | Flag | Flag-METTL8
55 / 35 — OCT4
55 / 35 — SOX2
55 / 35 — Flag-METTL8
35 — Actin

Fig4D IP

Input | IgG | anti-METTL8
KDa
55 / 35 — HC, METTL8

Fig4B

RA- RA+
cyto nucl cyto nucl
KDa
55 / 35 — METTL8
15 — H2A
55 / 35 — Actin

Fig3B

Day: 0 5 10 iPSCs
KDa
55 / 35 — METTL8
35 — Actin

Fig4E

KDa | Input | No probe | Sense | Anti-sense
55 / 35 — METTL8
35 — Actin

Fig4C

Input | IP: anti-Flag
Flag-GFP + +
Flag-METTL8 + +
KDa
55 / 35 / 25 — HC, Flag-METTL8, Flag-GFP

Fig5C

KDa | ctrl | Mettl8 KO
130 / 100 — MAPKBP1
55 / 35 — METTL8
35 — Actin

Fig6B

ctrl | Mettl8 KO
RA(Day): 0 1 2 4 0 1 2 4
KDa
70 / 55 / 35 — p-JNK
70 / 55 / 35 — JNK
130 / 100 — MAPKBP1
55 / 35 — OCT4
55 / 35 — METTL8
55 / 35 — Actin

Fig6C

ctrl | EB
ctrl | Mettl8 KO | ctrl | Mettl8 KO
KDa
55 / 35 — p-JNK
55 / 35 — JNK
55 / 35 — OCT4
55 / 35 — METTL8
35 — Actin

Fig5D

ctrl | Mettl8 KO
CHX(hr): 0 1 2 0 1 2
KDa
130 / 100 — MAPKBP1
55 / 35 — METTL8
55 / 35 — Actin

FigS6D

FigS6E

FigS6F

FigS6G

Figure S7. Uncropped images of Western blot

Table S4. List of primers sequences

Primers for qRT-PCR	
Gene	**Sequence (5'-3')**
Actin	Fw: CTGTCCCTGTATGCCTCTG
	Rev: ATGTCACGCACGATTTCC
Oct4	Fw: TCTTTCCACCAGGCCCCCGGCTC
	Rev: TGCGGGCGGACATGGGGAGATCC
Sox2	Fw: TAGAGCTAGACTCCGGGCGATGA
	Rev: TTGCCTTAAACAAGACCACGAAA
Nanog	Fw: CTCATCAATGCCTGCAGTTTTTCA
	Rev: CTCCTCAGGGCCCTTGTCAGC
Rex1	Fw: ACGAGGTGAGTTTTCCGAAC
	Rev: CCTCTGTCTTCTCTTGCTTC
Esg1	Fw: ATATCCCGCCGTGGGTGAAAGTTC
	Rev:ACTCAGCCATGGACTGGAGCATCC
Fbx15	Fw: GTTGGAATCTGCTTCTACAG
	Rev: CTTCACCAAGATTTCCGATG
Cdx2	Fw: CGAGCCCTTGAGTCCTGTGA
	Rev: AACCCCAGGGACAGAACCA
Hand1	Fw: GCCAAGGATGCACAAGCA
	Rev: GGGCTGCTGAGGCAACTC
Gata6	Fw: CTTGCGGGCTCTATATGAAACTCCAT
	Rev: TAGAAGAAGAGGAAGTAGGAGTCATAGGGACA
Ihh	Fw: ACGTGCATTGCTCTGTCAAGT
	Rev: CTGGAAAGCTCTCAGCCGGTT
Laminin B1	Fw: CCCCAATCTCTGTGAACCATG
	Rev: GCAATTTGCACCGACACTGA
Fgf5	Fw: TGCGTCCGCGATCCA
	Rev: TCAGGGCCACGTACCACTCT
Nestin	Fw: TGAGGGTCAGGTGGTTCTG
	Rev: AGAGCAGGGAGGGACATTC
Pax6	Fw: GCATGCAGAACAGTCACAGCGGA
	Rev: ACTCCCGTTTATACTGGGCTATTT
T	Fw: ATCACCAGCCACTGCTTTC
	Rev: CCATTACATCTTTGTGGTCGTTTC
Mixl1	Fw: ACTTTCCAGCTCTTTCAAGAGCC
	Rev: ATTGTGTACTCCCCAACTTTCCC
Mapkbp1	FW: TCCTGACCGTCCTACTCTGA
	REV: TTTCCTAGGCTCACCAAGGG
Mettl8	FW: CCACCCAGGAAGAGTCTCAG
	REV: GGTTACACCCATGGTCAGGA
Primers for CRISPR	
Name	**Sequence (5'-3')**
Mapkbp1 1	FW: caccgCGTTGACAATCATGTCATGC
	REV: aaacGCATGACATGATTGTCAACGc
Mapkbp1 2	FW: caccgCTTGCTTGTGACCCCCGATC
	REV: aaacGATCGGGGGTCACAAGCAAGc
Mettl8 1	FW: caccgGAAGTTGCATTTGCCGACTG
	REV: aaacCAGTCGGCAAATGCAACTTCc
Mettl8 2	FW: caccgTTGCATTTGCCGACTGAGGC
	REV: aaacGCCTCAGTCGGCAAATGCAAc

Biotin labelled probes for Mapkbp1 mRNA pull down	
Name	**Sequence (5'-3')**
Probe1	Sense: TTCTGTATCACGTCGTCGGG
	Antisense: CCCGACGTGATACAGAA
Probe2	Sense: TGCAAGAGAGCCCTAGTGTT
	Antisense: AACACTAGGGCTCTCTTGCA